Handedness resolved magneto-infrared spectroscopy of 2D and 3D Dirac materials

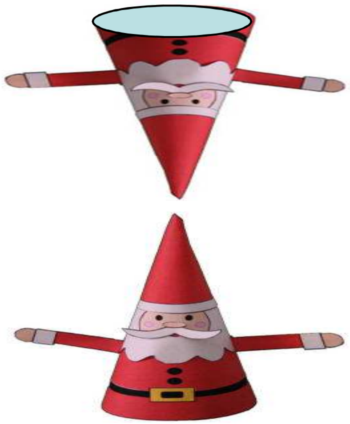

Alexey B. Kuzmenko
University of Geneva

20.01.17

Winter School
New Frontiers in 2D materials: Approaches & Applications

www.graphene-flagship.eu
GRAPHENE FLAGSHIP

UNIVERSITÉ DE GENÈVE

FNSNF
FONDS NATIONAL SUISSE DE LA RECHERCHE SCIENTIFIQUE

Acknowledgments

University of Geneva

Iris Crassee
Julien Levallois
Jean-Marie Poumirol
Pieter de Visser
Ievgeniia Nedoliuk
Michael Tran
Dirk van der Marel
Jérémie Teyssier

University of Zaragoza

Tetiana Slipchenko
Luis Martin-Moreno

University of Michigan

Ctirad Uher

LCNMI, Grenoble

Milan Orlita

ETHZ (Zurich)

Peter Q. Liu
Jérôme Faist

EPFL (Lausanne)

Michele Tamagnone
Clara Moldovan
Julien Perruiseau-Carrier
Juan Mosig

nanoGUNE (San-Sebastian)

Alexey Nikitin

www.graphene-flagship.eu
GRAPHENE FLAGSHIP

UNIVERSITÉ DE GENÈVE

FNSNF
FONDS NATIONAL SUISSE DE LA RECHERCHE SCIENTIFIQUE

Outline

- Handedness resolved magneto-infrared spectroscopy
- Anomalous magnetic circular dichroism (MCD) and valley-polarized magneto-absorption in bismuth
- Electrically controlled terahertz MCD and Faraday rotation in graphene

www.graphene-flagship.eu

GRAPHENE FLAGSHIP

UNIVERSITÉ DE GENÈVE

FNSNF

FONDS NATIONAL SUISSE DE LA RECHERCHE SCIENTIFIQUE

Outline

- Handedness resolved magneto-infrared spectroscopy

- Anomalous magnetic circular dichroism
  and valley-resolved magneto-absorption in bismuth

- Electrically controlled terahertz magneto-optical
  phenomena in graphene

www.graphene-flagship.eu

GRAPHENE FLAGSHIP

UNIVERSITÉ DE GENÈVE

FNSNF

FONDS NATIONAL SUISSE
DE LA RECHERCHE SCIENTIFIQUE

Why handedness resolved IR/THz spectroscopy?

- Magnetic-circular dichroism (MCD) is a very important parameter to identify magneto-optical transitions

- Measuring MCD in the far-infrared/THz directly is very challenging (no broadband waveplates, or photoelastic modulators)

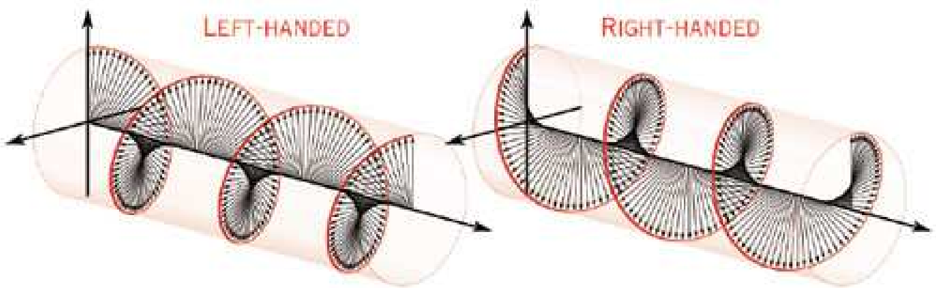

Image from: http://blog.atlasrfidstore.com/choose-right-rfid-antenna

Magneto-optical THz experiment in Geneva

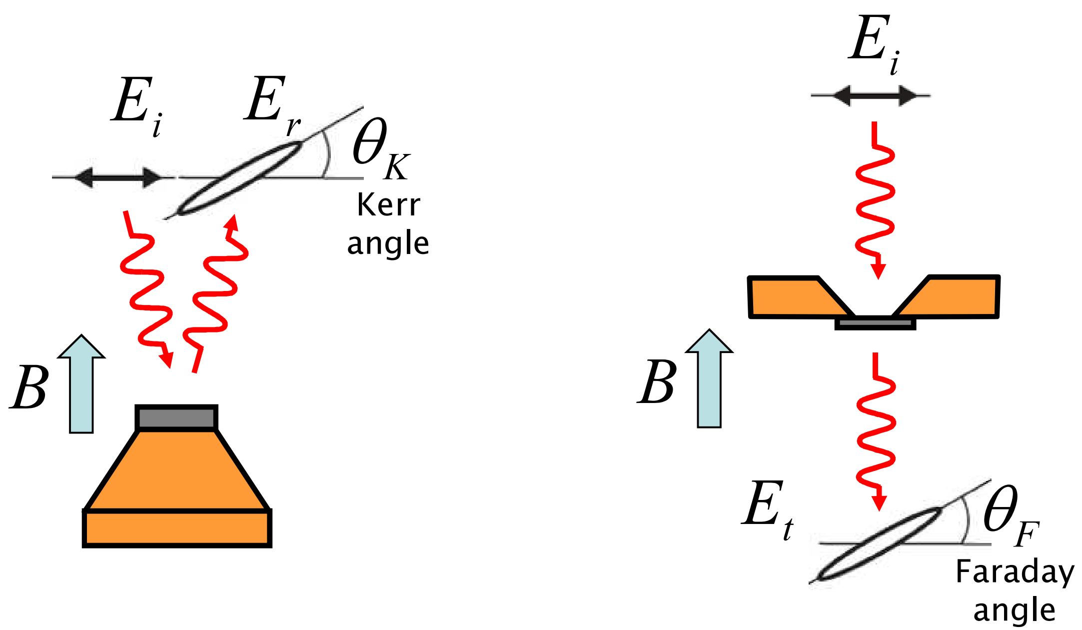

- FTIR or time-domain THz spectroscopy
- Magnetic field up to 7 T (superconducting coil)
- Transmission/reflection
- Faraday rotation / Kerr rotation

J. Levallois et al., Rev. Sci. Instrum. **86**, 033906 (2015)


ESAG

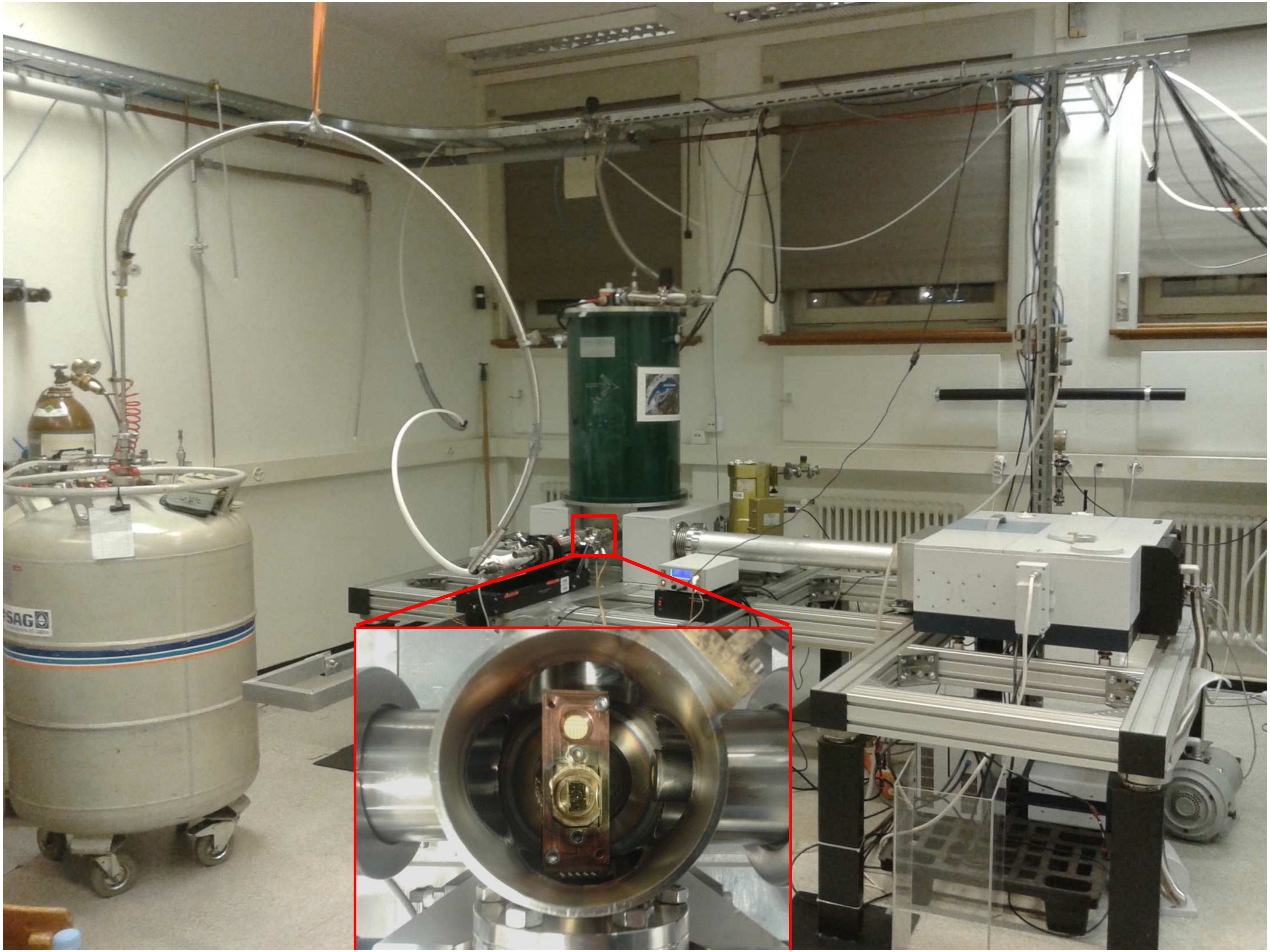
SAG

Magneto-optical Kramers-Kronig analysis (MOKKA)

Linear magneto-optical response

is determined by the transmission tensor:

$$\hat{t}(\omega, B) = \begin{pmatrix} t_{xx} & t_{xy} \\ -t_{xy} & t_{xx} \end{pmatrix}$$

L. Onsager, Phys. Rev. 37, 405 (1931)

or equivalently (in the circular basis): $t_{\pm} = t_{xx} \pm i t_{xy}$

We can directly measure:

Transmission (for linear polarized light) $T = \dfrac{|t_+|^2 + |t_-|^2}{2}$

Faraday rotation: $\theta_F = \dfrac{1}{2} Arg\left(\dfrac{t_-}{t_+}\right)$

Using a magneto-optical Kramers-Kronig analysis (MOKKA), we obtain:

Transmission (for circular polarized light): $T_+ = |t_+|^2 \quad T_- = |t_-|^2$

Ellipticity/MCD

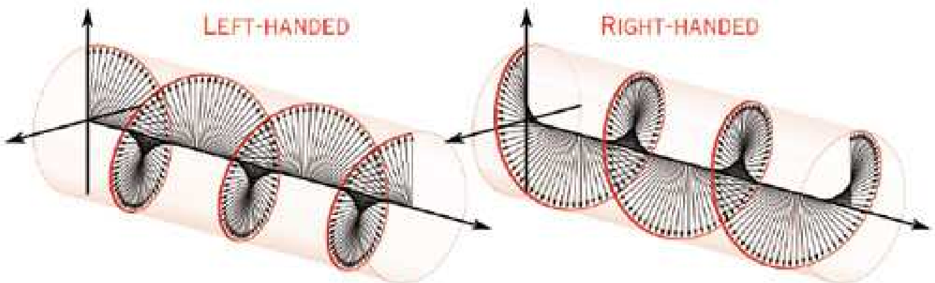

Image from: http://blog.atlasrfidstore.com/choose-right-rfid-antenna

J. Levallois et al., Rev. Sci. Instrum. 86, 033906 (2015)

Basic assumptions for MOKKA

1. Magneto-optical dielectric function $\epsilon(\omega,B)$ is:
   - local (q-independent)
   - isotropic in the plane $\perp$ B-field

2. Magnetic permeability $\mu(\omega,B)$ is negligible

3. Magnetoelectric (multiferroic, axionic etc.) terms are negligible

4. B-field and light-propagation are both normal to the sample surface

Parity relations for MO conductivity

Time-reversal symmetry is preserved:

$B = 0$

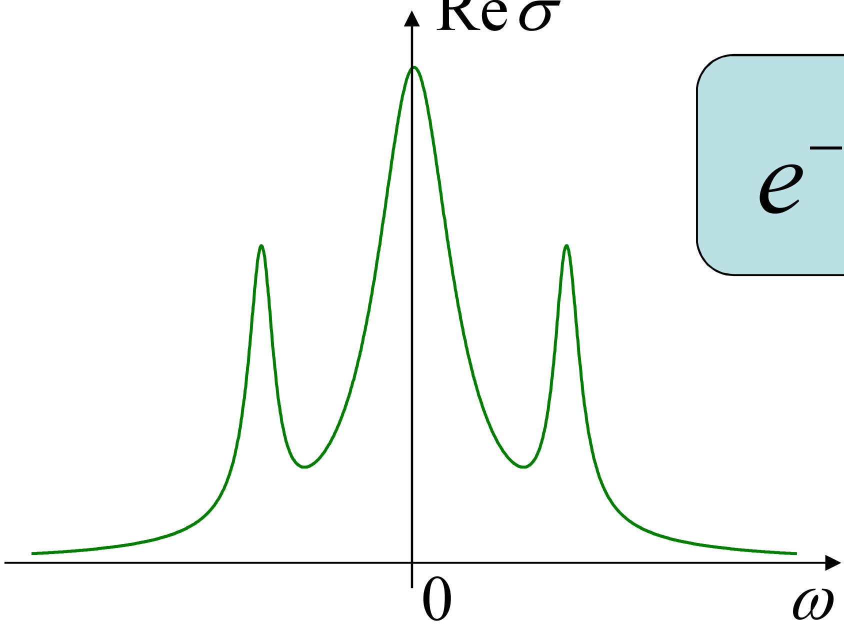

$$e^{-i\omega t}$$

Time-reversal symmetry is broken:

$B \neq 0$

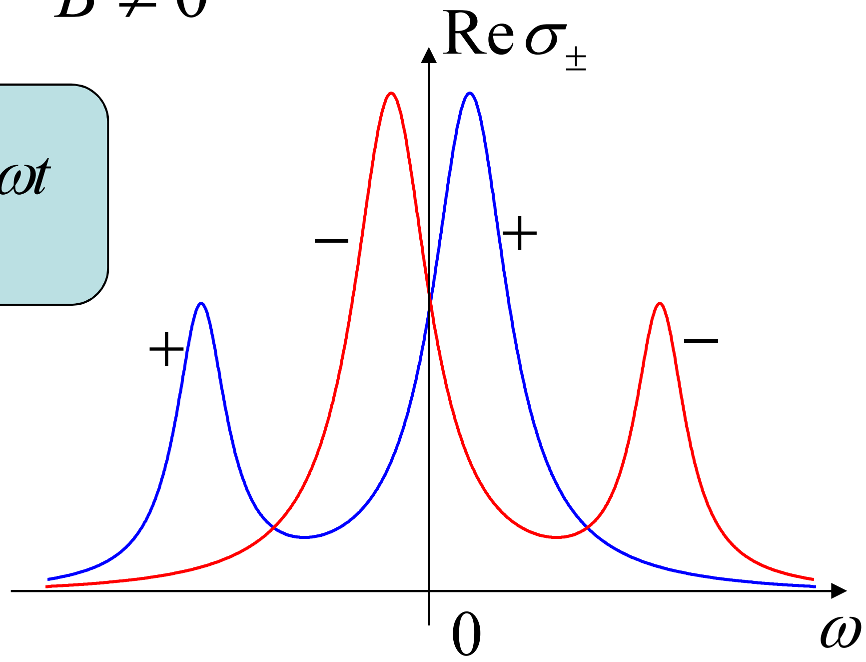

$$\sigma(-\omega) = \sigma^{*}(\omega)$$

$$\sigma_{\pm}(-\omega) = \sigma_{\mp}^{*}(\omega)$$

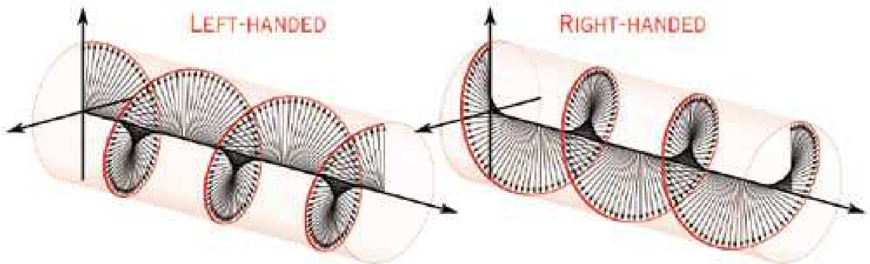

Image from: http://blog.atlasrfidstore.com/choose-right-rfid-antenna

Standard KK analysis of reflectivity

complex reflectivity (unknown)

$$r(\omega) = \sqrt{R(\omega)}e^{i\theta(\omega)}$$

real reflectivity (known)

$$R(\omega)$$

Consider the function:

$$f(\omega) = \ln r(\omega) = \ln \underbrace{\sqrt{R(\omega)}}_{\text{known}} + \underbrace{i\theta(\omega)}_{\text{unknown}}$$

Does not apply to magneto-optics !

If f is analytic (meromorphic (e.g. for normal reflectivity from a bulk sample) then the KK relation applies:

$$\theta(\omega) = -\frac{1}{\pi}\wp\int_{-\infty}^{\infty}\frac{\ln\sqrt{R(x)}}{x-\omega}dx + \pi$$

Since $R(-\omega) = R(\omega)$ $\Rightarrow$ $\theta(\omega) = -\frac{\omega}{\pi}\wp\int_{0}^{\infty}\frac{\ln R(x)}{x^2-\omega^2}dx + \pi$

This proves the theorem: $\boxed{R(\omega) \text{ in } (0, +\infty) \text{ determines } \underline{\text{uniquely}}\ r(\omega)}$

For a reliable KK analysis one has to measure in a broad range and/or use additional measurements, such as ellipsometry

F.C. Jahoda, Phys. Rev. 107, 1261 (1957)

MOKKA (direct integration)

complex reflectivity (unknown)

$$r_\pm(\omega) = \sqrt{R_\pm(\omega)}e^{i\theta_\pm(\omega)}$$

real reflectivity (known)

$$R(\omega) = \frac{R_+(\omega) + R_-(\omega)}{2}$$

Kerr angle (known)

$$\theta_K(\omega) = \frac{\theta_-(\omega) - \theta_+(\omega)}{2}$$

Consider the function:

$$f(\omega) = \ln\left(\frac{r_-(\omega)}{r_+(\omega)}\right) = \frac{1}{2}\ln \underbrace{c(\omega)}_{\text{unknown}} + 2i\underbrace{\theta_K(\omega)}_{\text{known}}$$

where $c(\omega) = \dfrac{R_-(\omega)}{R_+(\omega)}$ is circular-dichroism ratio

1st KK relation:

$$c(\omega) = \exp\left\{\frac{8\omega}{\pi}\wp\int_0^\infty \frac{\theta_K(x)}{x^2-\omega^2}dx\right\} \Rightarrow R_+(\omega) = \frac{2R(\omega)}{1+c(\omega)} \Rightarrow R_-(\omega) = \frac{2c(\omega)R(\omega)}{1+c(\omega)}$$

2nd KK relation: $\theta_\pm(\omega) = -\dfrac{1}{\pi}\wp\displaystyle\int_{-\infty}^{\infty}\frac{\ln\sqrt{R_\pm(x)}}{x-\omega}dx + \pi$

Since $R_\pm(-\omega) = R_\mp(\omega)$

$$\Rightarrow \theta_\pm(\omega) = -\frac{\omega}{\pi}\wp\int_0^\infty \frac{\ln\sqrt{R_+(x)R_-(x)}}{x^2-\omega^2}dx + \pi \mp \theta_K(\omega)$$

This proves the theorem: $R(\omega)$ and $\theta_K(\omega)$ in $(0, +\infty)$ determine uniquely $r_\pm(\omega)$

J. Levallois et al., Rev. Sci. Instrum. 86, 033906 (2015)

Polarimetric experiment
"fixed polarizer, rotating analyser" *

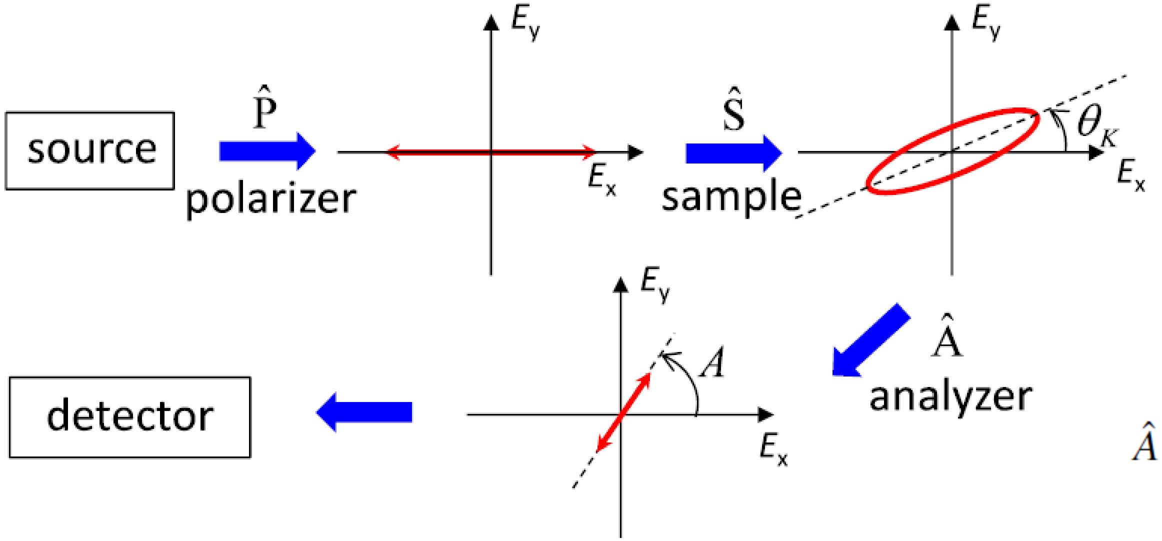

Jones matrices

$$\hat{P} = t_P \begin{pmatrix} 1 & 0 \\ 0 & 0 \end{pmatrix}$$

$$\hat{S} = \begin{pmatrix} r_{xx} & r_{xy} \\ -r_{xy} & r_{xx} \end{pmatrix}$$

$$\hat{A} = t_A \begin{pmatrix} \cos^2 A & \cos A \sin A \\ \cos A \sin A & \sin^2 A \end{pmatrix}$$

$$I_A = C_A \frac{R + \tilde{R}\cos(2A - 2\theta_K)}{2}$$

where

$$R(\omega) = \frac{R_+(\omega) + R_-(\omega)}{2}$$

$$\tilde{R}(\omega) = \sqrt{R_+(\omega)R_-(\omega)}$$

Ellipsometry at normal incidence !

* The same applies to the case «rotating polarizer, fixed analyzer»

Extracting reflectivity and Kerr angle*

$$I_A = C_A \frac{R + \tilde{R}\cos(2A - 2\theta_K)}{2}$$

where

$$R(\omega) = \frac{R_+(\omega) + R_-(\omega)}{2}$$

$$\tilde{R}(\omega) = \sqrt{R_+(\omega)R_-(\omega)}$$

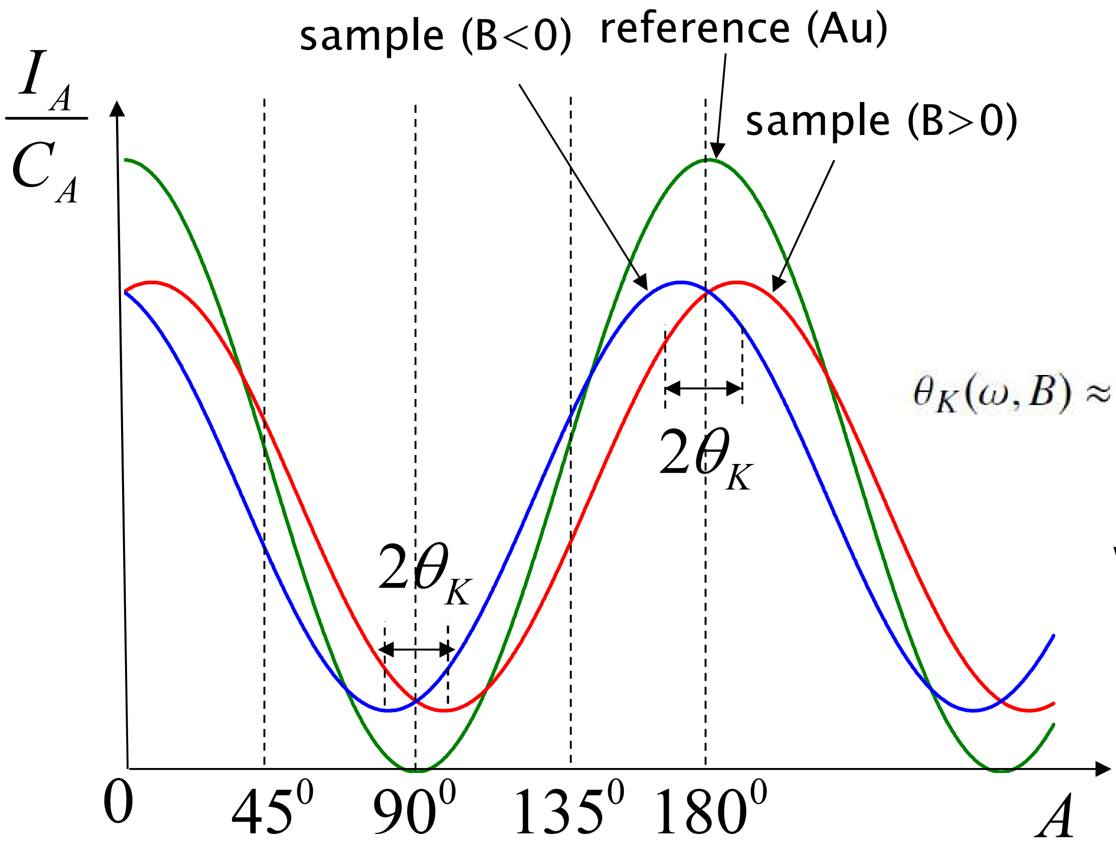

Fast protocol
(accurate if $\theta_K < 0.2$ rad)

$$R(\omega, B) \approx \frac{I_0(\omega, B)}{I_{0,ref}(\omega, B)}$$

$$\theta_K(\omega, B) \approx \frac{1}{8}\left[\frac{\rho_{+45}(\omega, B)}{\rho_{+45,ref}(\omega, B)} - \frac{\rho_{-45}(\omega, B)}{\rho_{-45,ref}(\omega, B)}\right]$$

where $\rho_{\pm 45}(\omega, B) = \frac{I_{\pm 45}(\omega, +B)}{I_{\pm 45}(\omega, -B)}$

only measurements
at A=0, 45 and -45
needed !

* The same applies to the case of transmission and Faraday angle

J. Levallois et al., Rev. Sci. Instrum. 86, 033906 (2015)

Advantages of MOKKA

- broadband (based on polarizers only)
- can be applied at high magnetic fields (polarizers are fixed)

The first Faraday rotation
spectroscopic measurement at 30 T

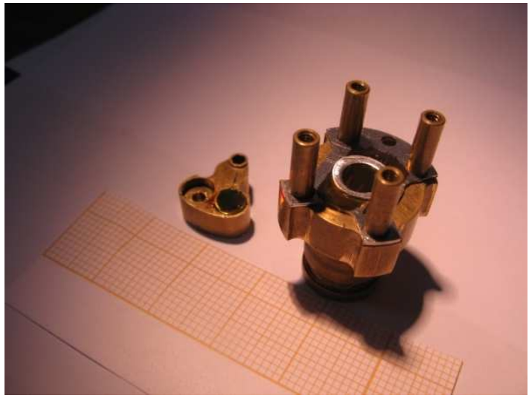

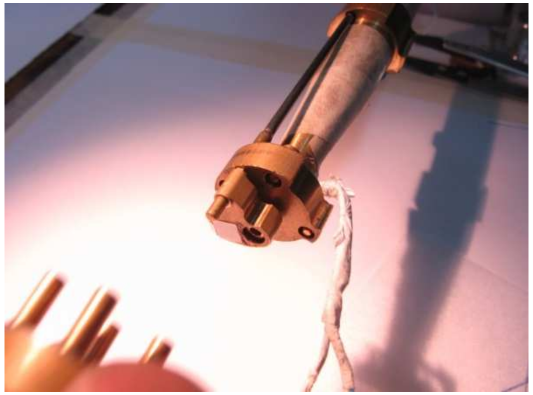

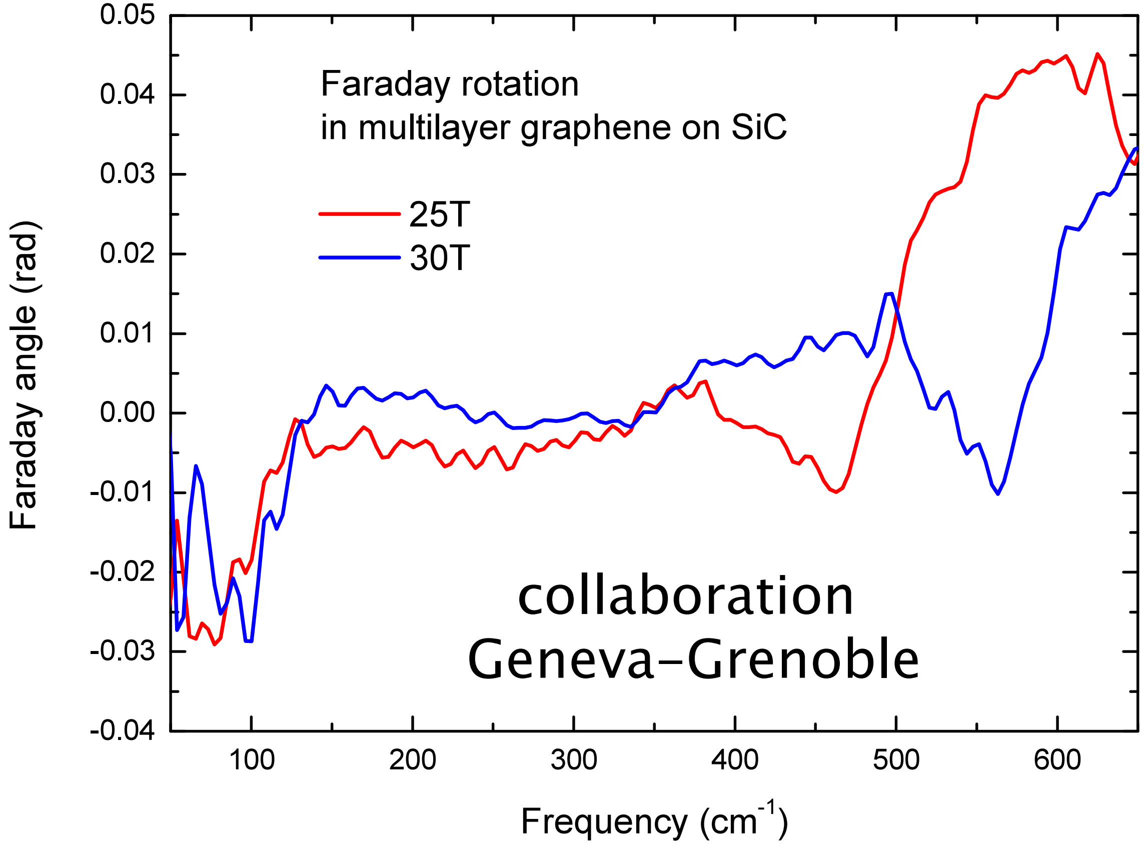

Advantages of MOKKA

J. Levallois et al., Rev. Sci. Instrum. 86, 033906 (2015)

Outline

- Handedness resolved magneto-infrared spectroscopy
- Anomalous magnetic circular dichroism
  and valley-resolved magneto-absorption in bismuth
- Electrically controlled terahertz magneto-optical
  phenomena in graphene

www.graphene-flagship.eu
GRAPHENE FLAGSHIP

UNIVERSITÉ DE GENÈVE

FNSNF
FONDS NATIONAL SUISSE DE LA RECHERCHE SCIENTIFIQUE

In the beginning was the Bismuth…

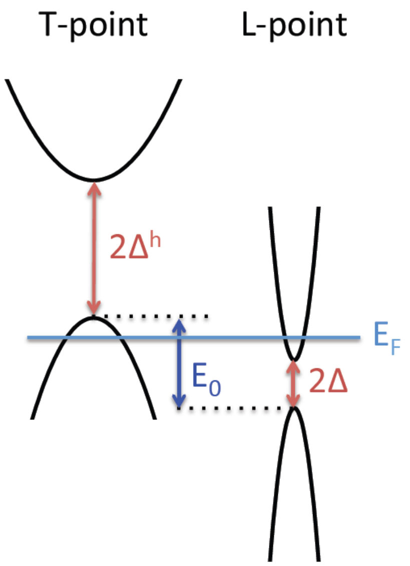

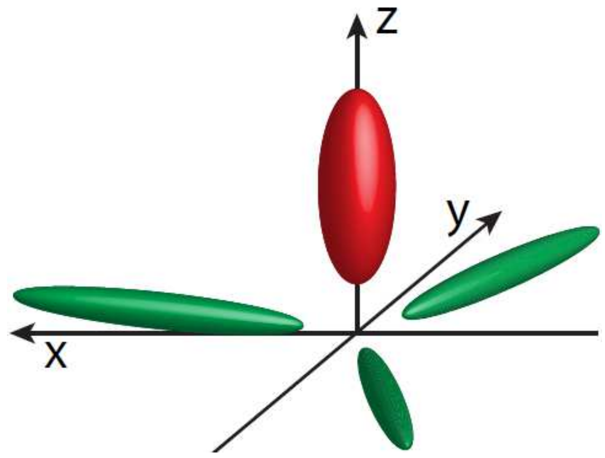

Image from: Z. Zhu et al. PRB 84, 115137 (2011).

- Ultralow-density 3D-Dirac semimetal
- Strong spin-orbit coupling
- Huge band-mass anisotropy (> 200)
- Topological insulator when alloyed with Sb
- …

Table I. Chronological table of phenomena discovered first in bismuth.

Year	Discovery
1778	Diamagnetism (Brugmans; named by Faraday in 1845)
1821	Seebeck effect
1886	Nernst effect (Ettingshausen and Nernst)
1928	Kapitza's law of magnetoresistance
1930	Shubnikov–de Haas effect
1930	de Haas–van Alphén effect
1955	Cyclotron resonance in metals (Galt)
1963	Oscillatory magnetostriction (Green and Chandrasekhar)

Table from: Fuseya et al. JPSJ 84, 012001 (2015)

Numerous reviews are available…

Bismuth crystals

Very soft material, cleaved in liquid nitrogen, always on the trigonal plane

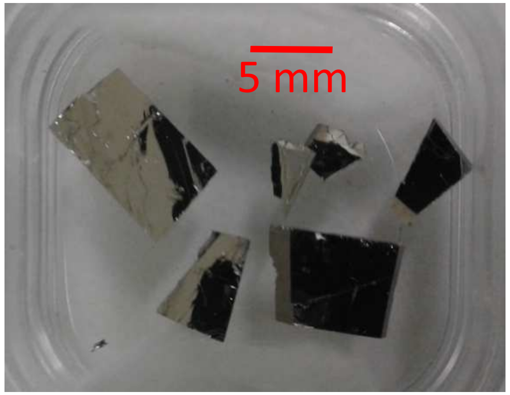

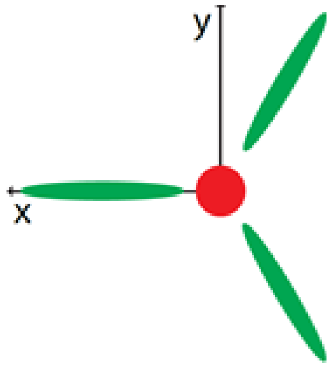

- Atomically flat surface
- Steps 0.4, 0.8 and 1.2nm (1/3, 2/3 and 1 unit-cell)

AFM topography

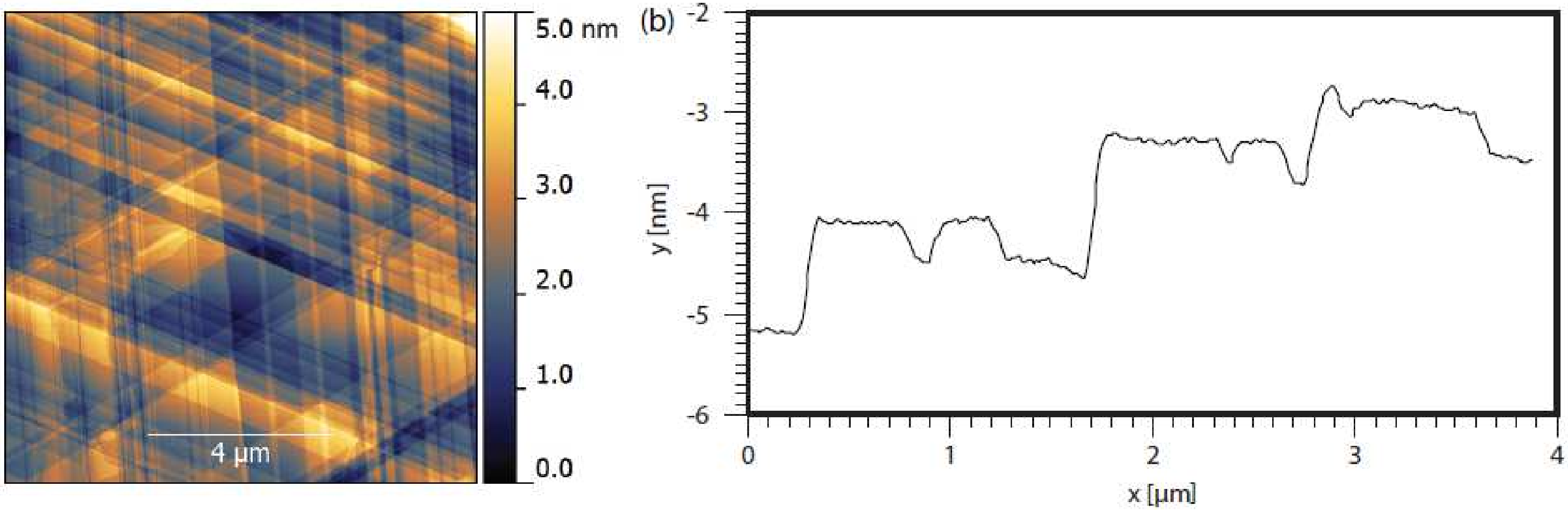

P.J. de Visser, J. Levallois *et al.* Phys. Rev. Lett. 117, 017402 (2016)

Far-IR reflectivity + Kerr rotation on bismuth

Magneto-reflectivity

Kerr rotation

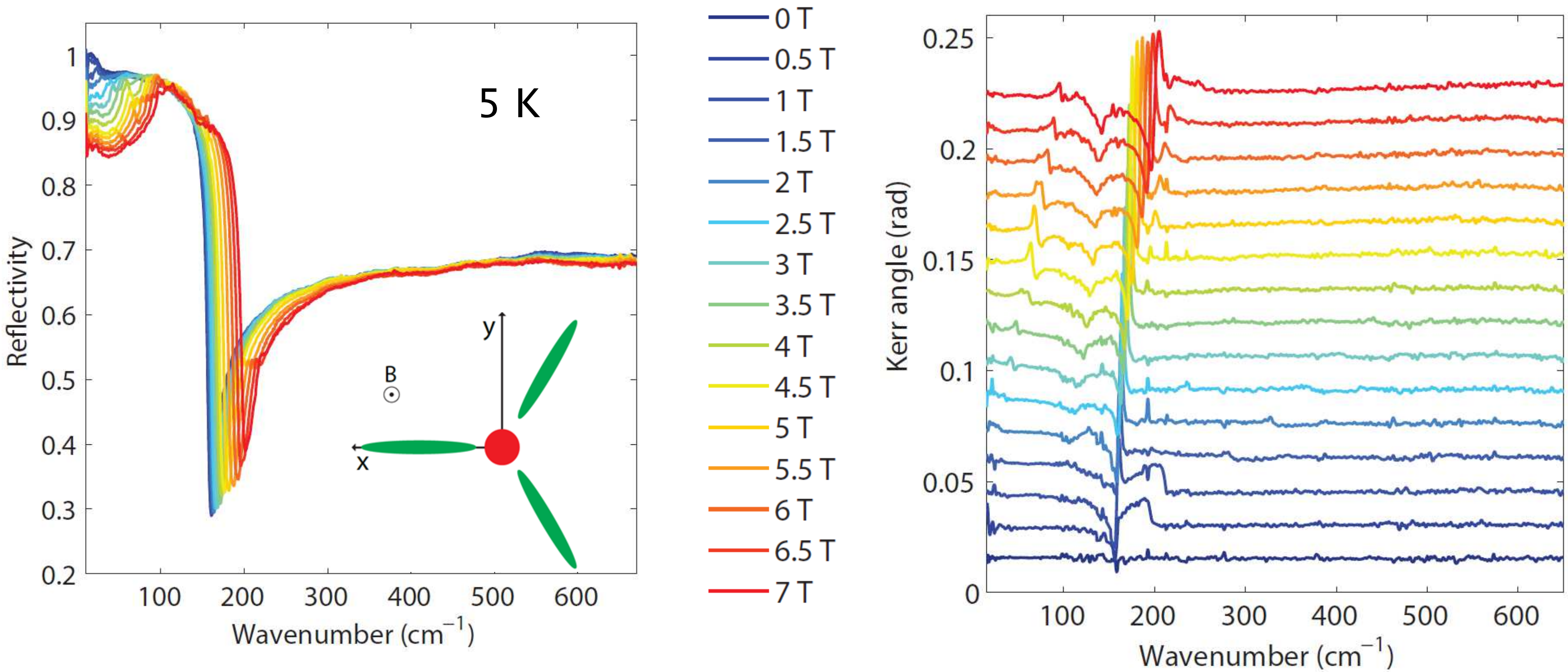

Why not done before ?

- Spectroscopic (FTIR) experiments never combined with Kerr rotation
- Handedness-resolved experiments only at fixed (laser) wavelengths

P.J. de Visser, J. Levallois *et al.* Phys. Rev. Lett. 117, 017402 (2016)

Handedness-resolved magneto-optical conductivity of bismuth (from MOKKA)

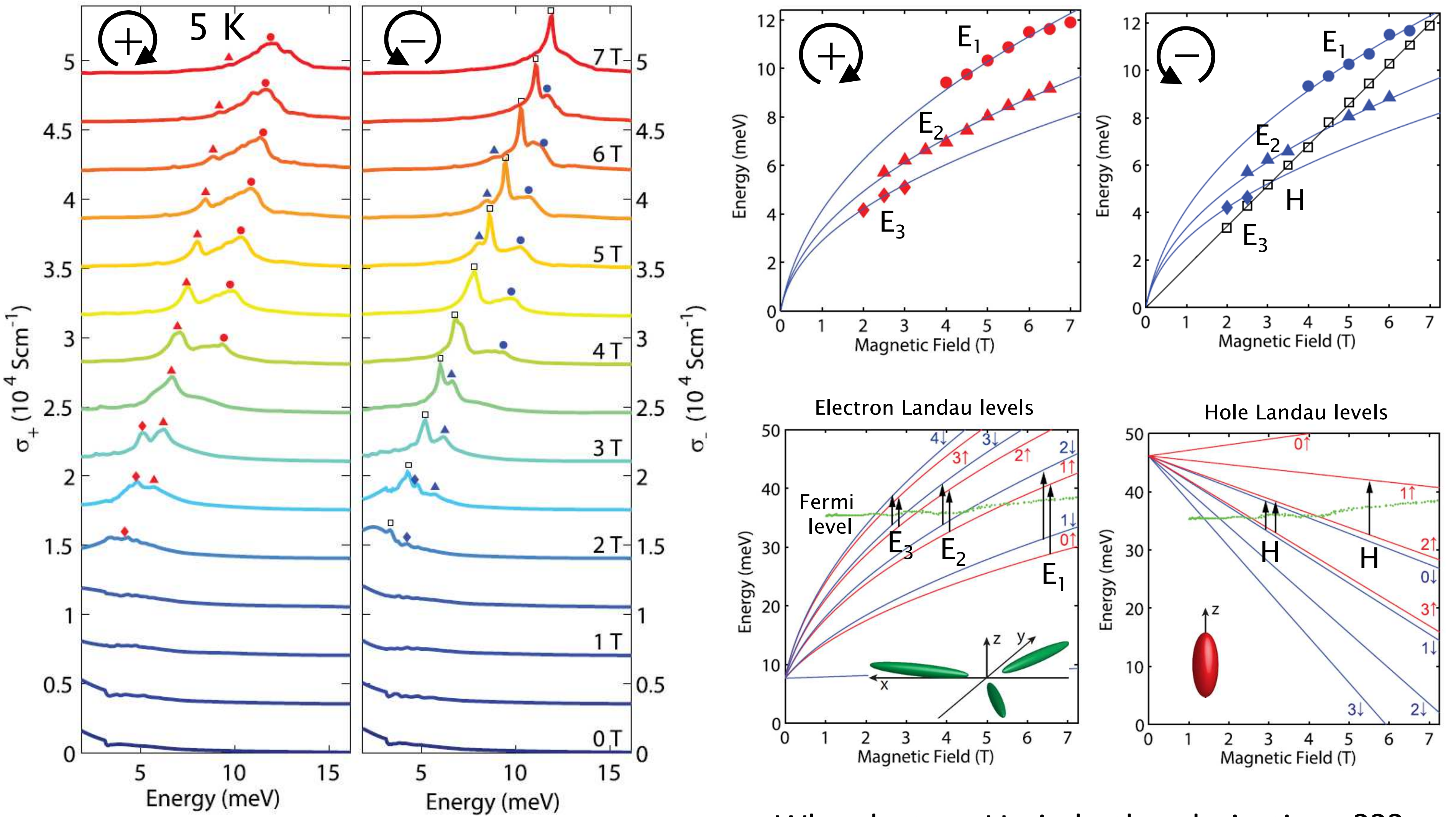

Why electron LLs in both polarizations ???

P.J. de Visser, J. Levallois *et al.* Phys. Rev. Lett. 117, 017402 (2016)

Magnetic circular dichroism (MCD) in bismuth

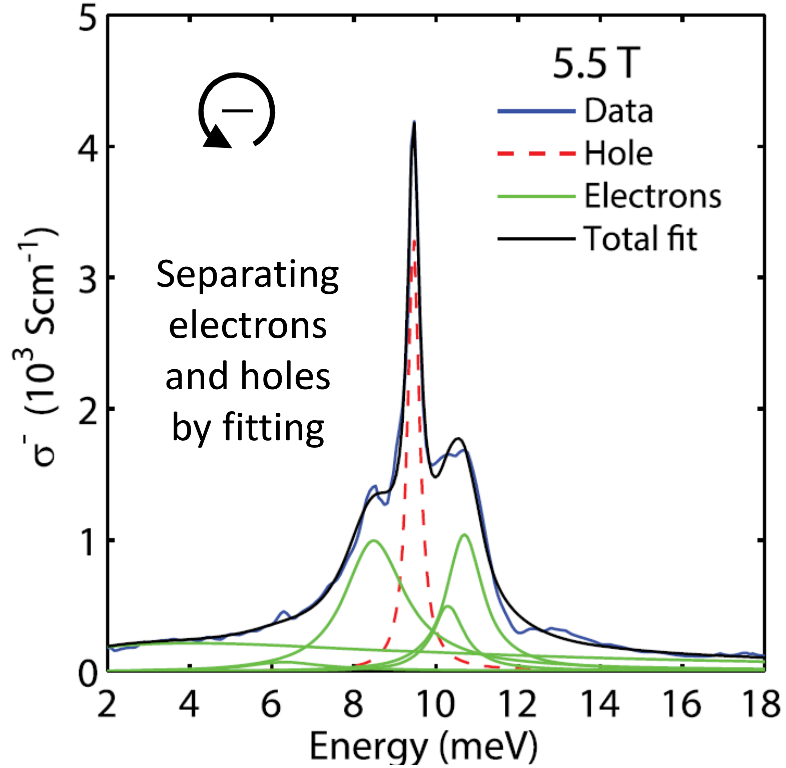

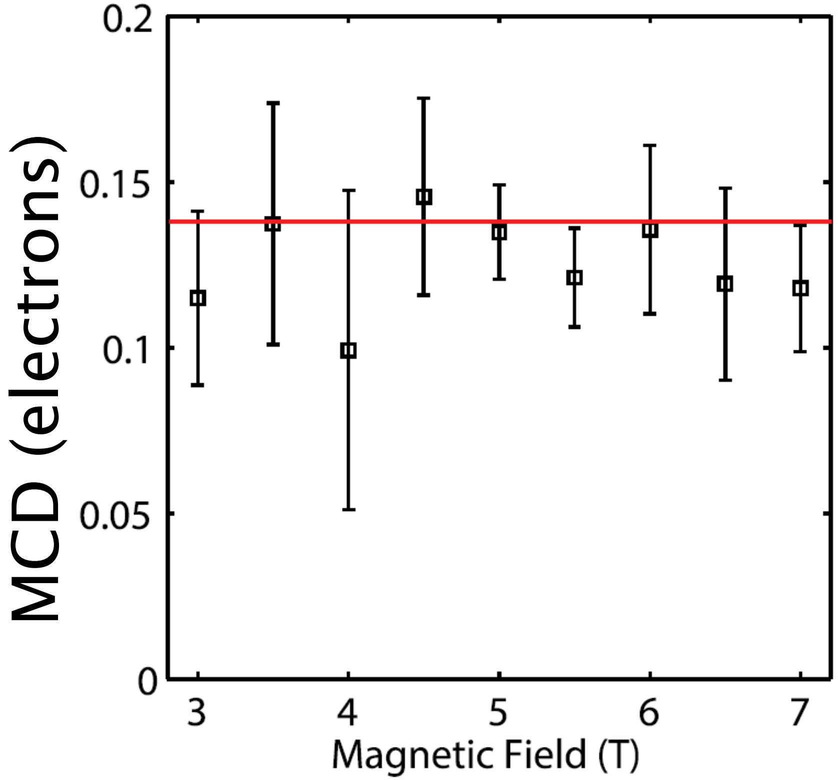

$$\mathrm{MCD} = \frac{\sigma_+ - \sigma_-}{\sigma_+ + \sigma_-} = \begin{cases} 100\% & \text{(holes)} \\ 13 \pm 1\% & \text{(electrons)} \end{cases}$$

Hugely suppressed for electrons !

P.J. de Visser, J. Levallois *et al.* Phys. Rev. Lett. 117, 017402 (2016)

3D Dirac gapped Hamiltonian and LLs in Bi

$$H_e(B) = \begin{bmatrix} \Delta & 0 & i\hbar v_z k_z & i\frac{\sqrt{2}}{l_B}\hbar v a^- \\ 0 & \Delta & i\frac{\sqrt{2}}{l_B}\hbar v a^+ & -i\hbar v_z k_z \\ -i\hbar v_z k_z & -i\frac{\sqrt{2}}{l_B}\hbar v a^- & -\Delta & 0 \\ -i\frac{\sqrt{2}}{l_B}\hbar v a^+ & i\hbar v_z k_z & 0 & -\Delta \end{bmatrix}$$

$$v = (\Delta/m_c)^{1/2}$$
$$v_z = (\Delta/m_z)^{1/2}$$
$$l_B = (\hbar/eB)^{1/2}$$

– magnetic length

Ladder operators: $k_x + ik_y \to \frac{l_B}{\sqrt{2}}a^+$, $k_x - ik_y \to \frac{l_B}{\sqrt{2}}a^-$

Landau levels:

$$E_e(n,s,B) = \sqrt{\Delta^2 + 2\Delta\left(n + \frac{1}{2} + s\right)\frac{\hbar e B}{m_c}} + sg\mu_B B$$

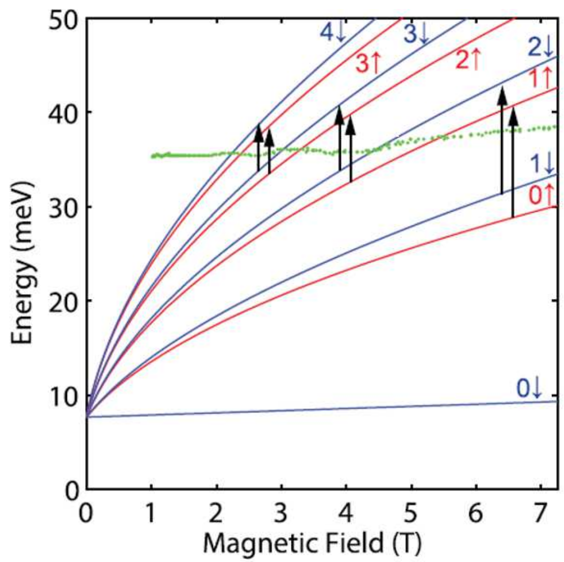

Model agrees perfectly with Nerst, dHvA, SdH… effects

Therefore LLs, $E_F(B)$, DoS(B) are for sure correct

M. H. Cohen and E. I. Blount, Phil. Mag. **5**, 115 (1960).
Z. Zhu et al. PRB 84, 115137 (2011).

3D Dirac gapped Hamiltonian and LLs in Bi

Landau levels:

$$E_e(n,s,B) = \sqrt{\Delta^2 + 2\Delta\left(n + \frac{1}{2} + s\right)\frac{\hbar e B}{m_c}} + s g' \mu_B B$$

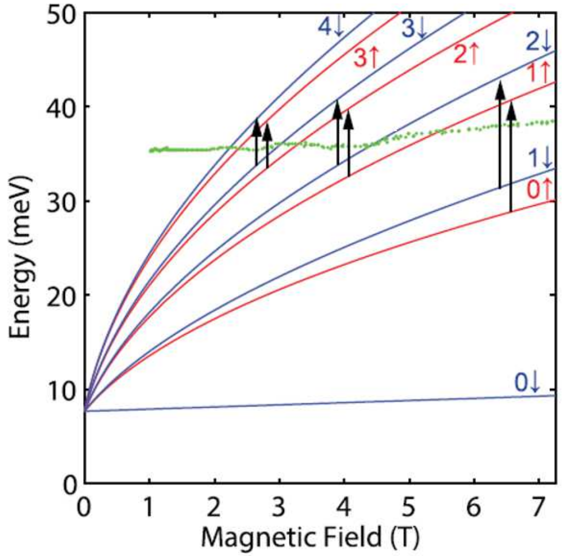

Theory:

Selection rules for LL transitions::

$\Delta s = 0$

RH circular: $\Delta n = +1$ $\quad \sigma_+ \neq 0$

LH circular: $\Delta n = -1$ $\quad \sigma_- = 0$

$\mathrm{MCD} = 100\%$

Experiment: $\mathrm{MCD} = 13\%$

Does not explain the suppression of MCD !!!

Mechanism of electron–MCD reduction in Bi

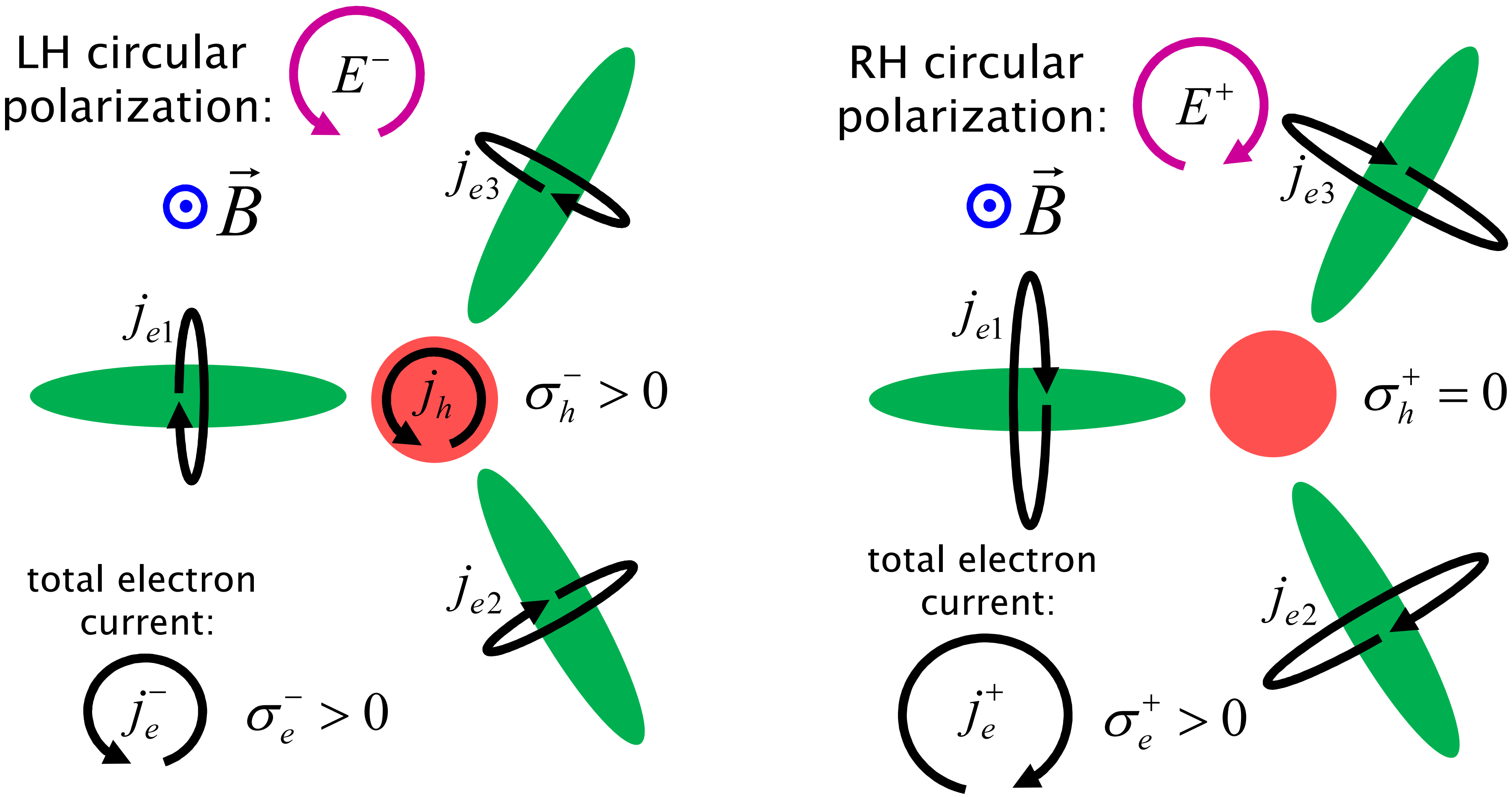

$$MCD(\text{holes}) = \frac{\sigma_h^+ - \sigma_h^-}{\sigma_h^+ + \sigma_h^-} = 100\%$$

$$MCD(\text{electr.}) = \frac{\sigma_e^+ - \sigma_e^-}{\sigma_e^+ + \sigma_e^-} << 100\%$$

Anisotropic mass as anisotropic metric

$\alpha = (m_x/m_y)^{1/2}$ - anisotropy parameter (≈ 15 in Bi)

Mass anisotropy is equivalent to <u>anisotropic spatial metric</u>

$$\tilde{x} = \alpha^{-1/2} x \ , \ \tilde{y} = \alpha^{1/2} y$$

$$\tilde{k}_x = \alpha^{1/2} k_x \ , \ \tilde{k}_y = \alpha^{-1/2} k_y$$

Anisotropic problem can be mapped isotropic problem:

$$\tilde{k}_x + i\tilde{k}_y \rightarrow \frac{l_B}{\sqrt{2}} \tilde{a}^+ \ , \ \tilde{k}_x + i\tilde{k}_y \rightarrow \frac{l_B}{\sqrt{2}} \tilde{a}^-$$

LL energies thus remain the same: $\tilde{E}_n(B, k_z) = E_n\,(B, k_z)$

But LL wavefunctions are scaled :

$$\tilde{\Psi}_n(B, x, y, k_z) = \Psi_n\left(B, \alpha^{-1/2} x, \alpha^{1/2} y, k_z\right)$$

Magneto-optical conductivity (in one valley):

$$\hat{\sigma}_{e1} = \begin{pmatrix} \alpha^{-1} s_{xx} & s_{xy} \\ -s_{xy} & \alpha s_{xx} \end{pmatrix}$$

Adding three anisotropic pockets together...

One pocket conductivity:

$$\alpha = \sqrt{\frac{m_x}{m_y}}$$

$$\hat{\sigma}^{e1} = \begin{pmatrix} \tilde{\sigma}_{xx} & \tilde{\sigma}_{xy} \\ -\tilde{\sigma}_{xy} & \tilde{\sigma}_{yy} \end{pmatrix} = \begin{pmatrix} \alpha^{-1} s_{xx} & s_{xy} \\ -s_{xy} & \alpha s_{xx} \end{pmatrix}$$

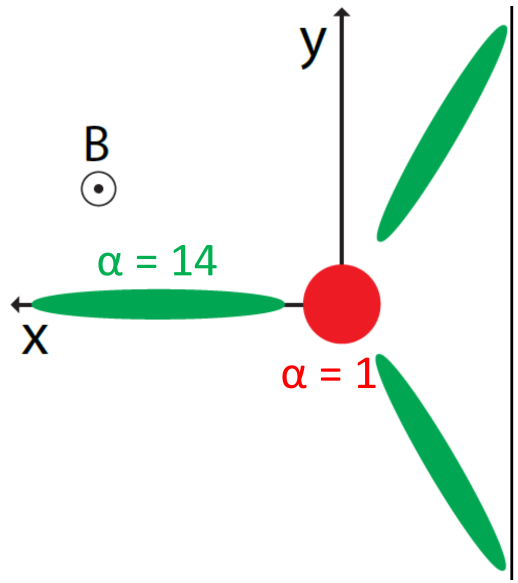

Add three pockets:

$$\hat{\sigma}^{tot} = \hat{\sigma}^{e1} + \hat{\sigma}^{e2} + \hat{\sigma}^{e3} = \hat{\sigma}^{e1} + \hat{R}\hat{\sigma}^{e1}\hat{R}^{-1} + \hat{R}^{-1}\hat{\sigma}^{e1}\hat{R}$$

$$\mathrm{MCD} = \frac{\sigma_e^+ - \sigma_e^-}{\sigma_e^+ + \sigma_e^-} = \frac{2}{\alpha + \alpha^{-1}} \approx 13.8\%$$

Agrees perfectly with experiment !

P.J. de Visser, J. Levallois *et al.* Phys. Rev. Lett. 117, 017402 (2016)

Valley-selective absorption in bismuth

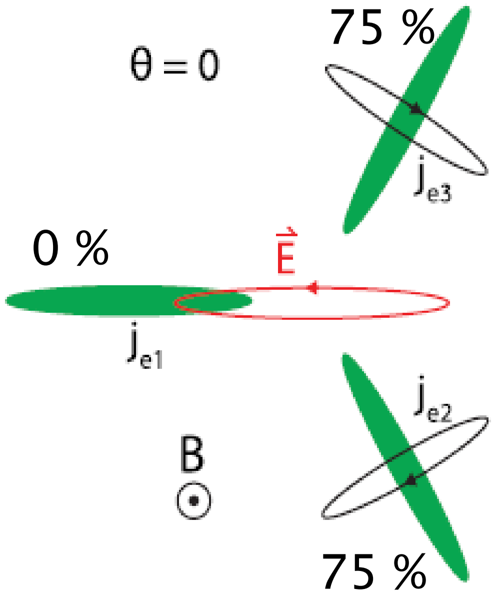

P.J. de Visser, J. Levallois *et al.* Phys. Rev. Lett. 117, 017402 (2016)

Valley-selective absorption in bismuth

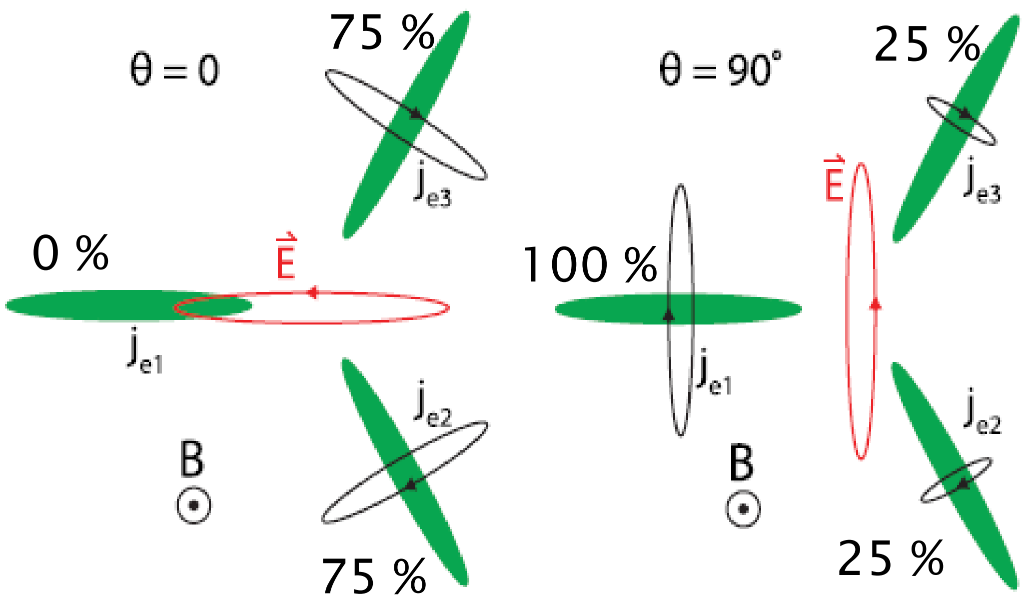

P.J. de Visser, J. Levallois *et al.* Phys. Rev. Lett. 117, 017402 (2016)

Valley-selective absorption in bismuth

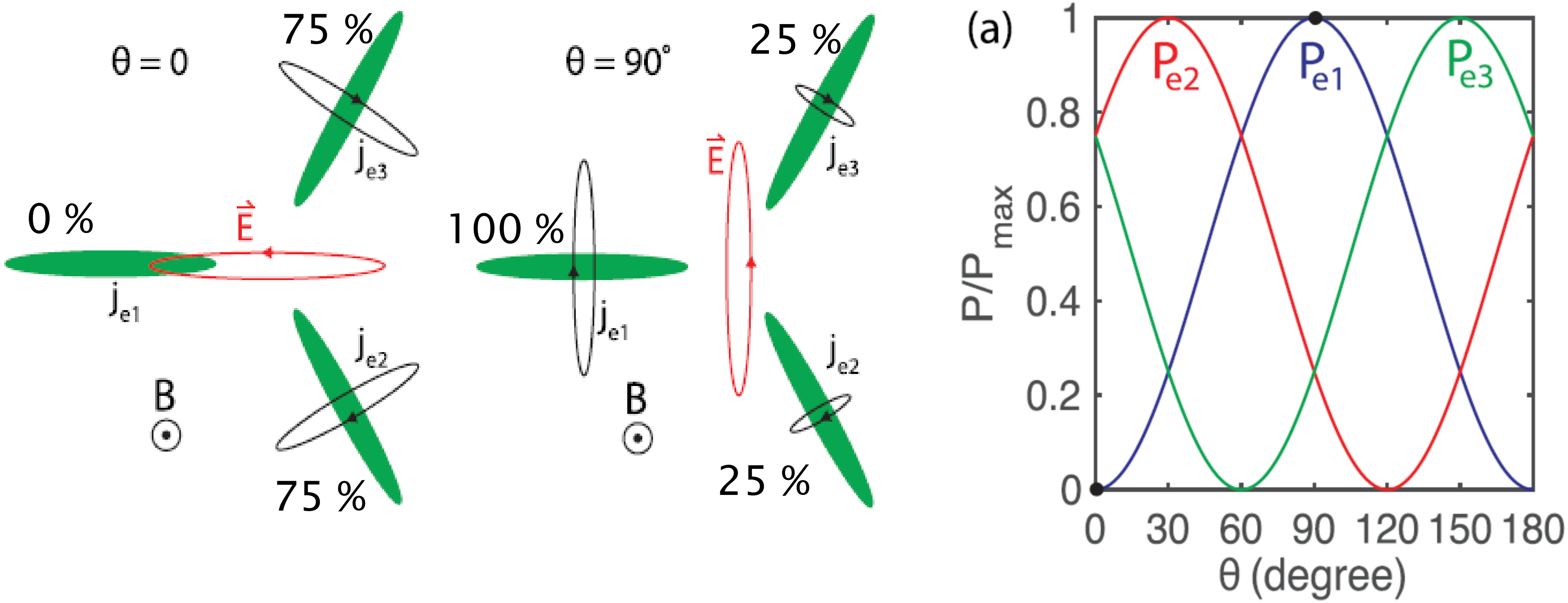

- Elliptical light absorbed differently in different valleys
- Valley are selected by the azimuth angle

P.J. de Visser, J. Levallois *et al.* Phys. Rev. Lett. 117, 017402 (2016)

Valley-selective absorption in bismuth

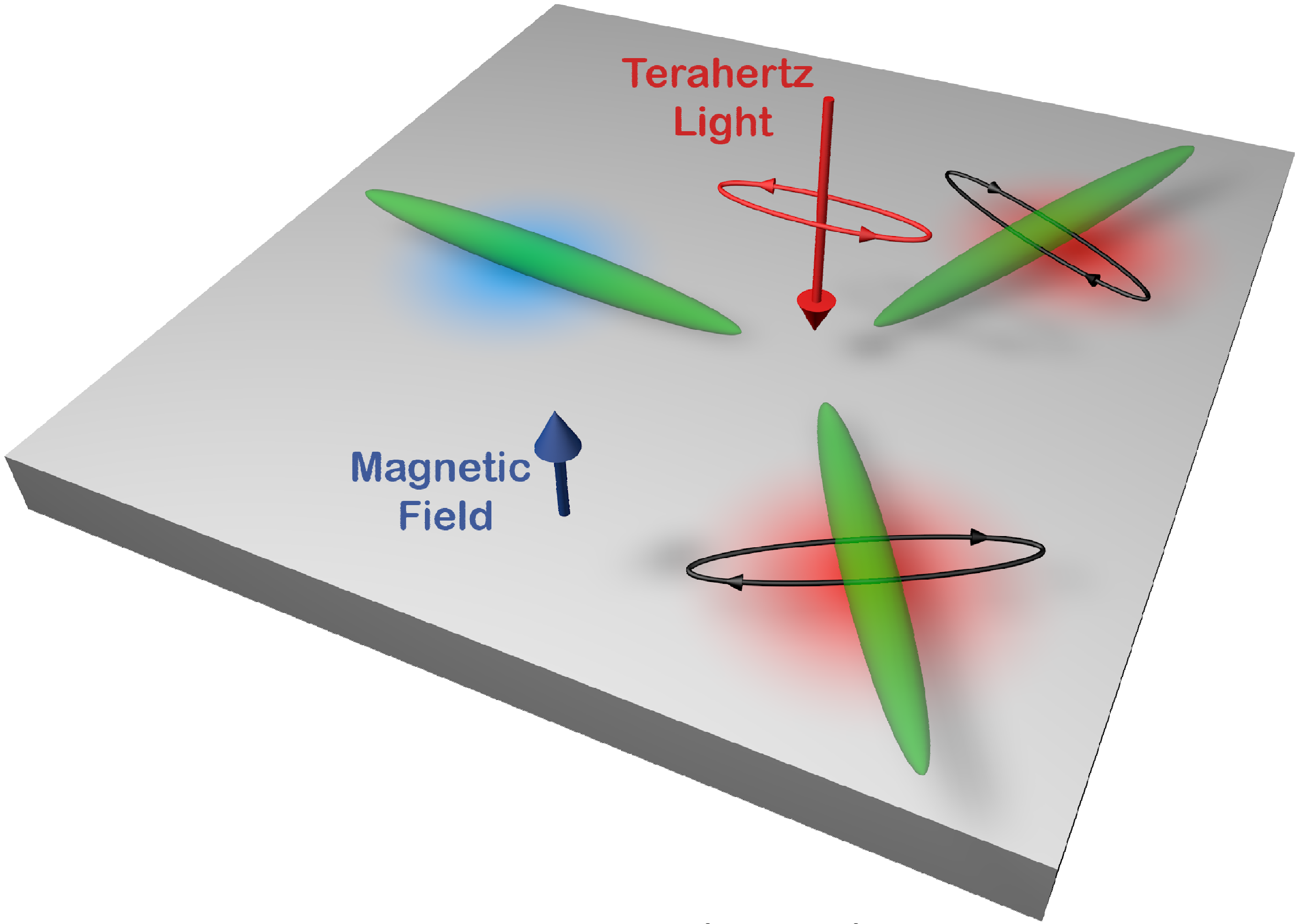

Mean-free path up to millimeters (at 5 K)

A new playground for valleytronics ?

P.J. de Visser, J. Levallois *et al.* Phys. Rev. Lett. 117, 017402 (2016)

Valley-selective absorption in TMDs

- Spin-polarized valence band (due to SO interaction)
- Valley-selective excitation with circularly polarised light

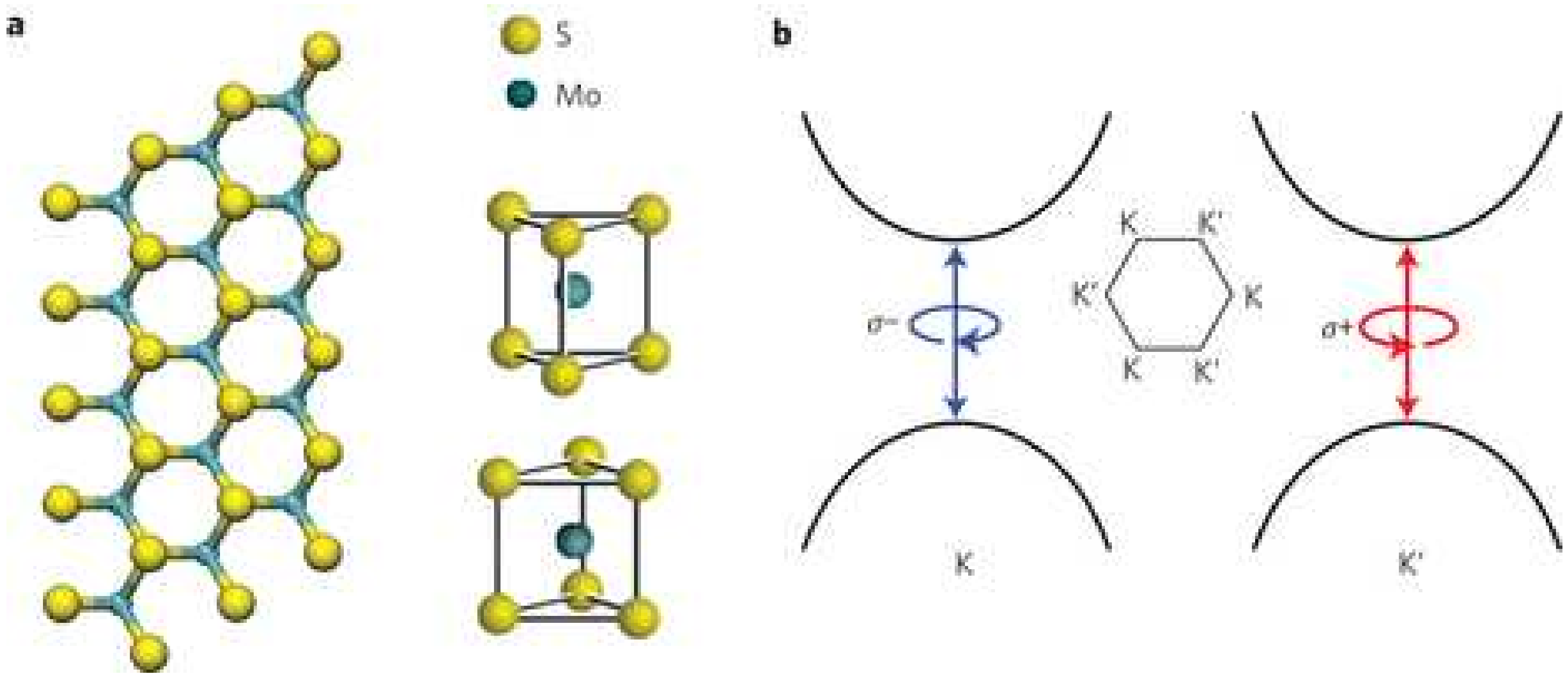

H. Zeng et al. Nature Nano. 7, 490 (2012)

Outline

- Handedness resolved magneto-infrared spectroscopy
- Anomalous magnetic circular dichroism and valley-resolved magneto-absorption in bismuth
- Electrically controlled terahertz magneto-optical phenomena in graphene

www.graphene-flagship.eu
GRAPHENE FLAGSHIP

UNIVERSITÉ DE GENÈVE

FNSNF
FONDS NATIONAL SUISSE DE LA RECHERCHE SCIENTIFIQUE

Graphene field-effect transistor (g-FET) for THz wave manipulation

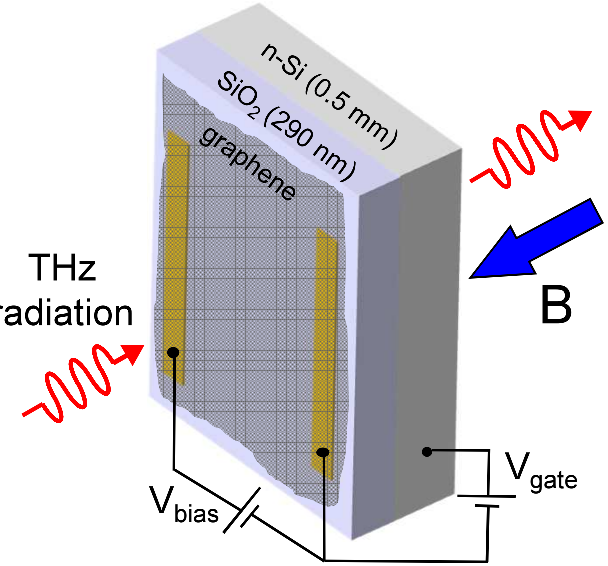

- large area needed for THz
- substrate SiO_2(300 nm)/Si
- Low-doped Si for THz transparency
- CVD graphene transferred from Cu
- evaporated Au/Ti contacts
- annealed by high current in vacuum
- simultaneous magneto-optics and magneto-transport

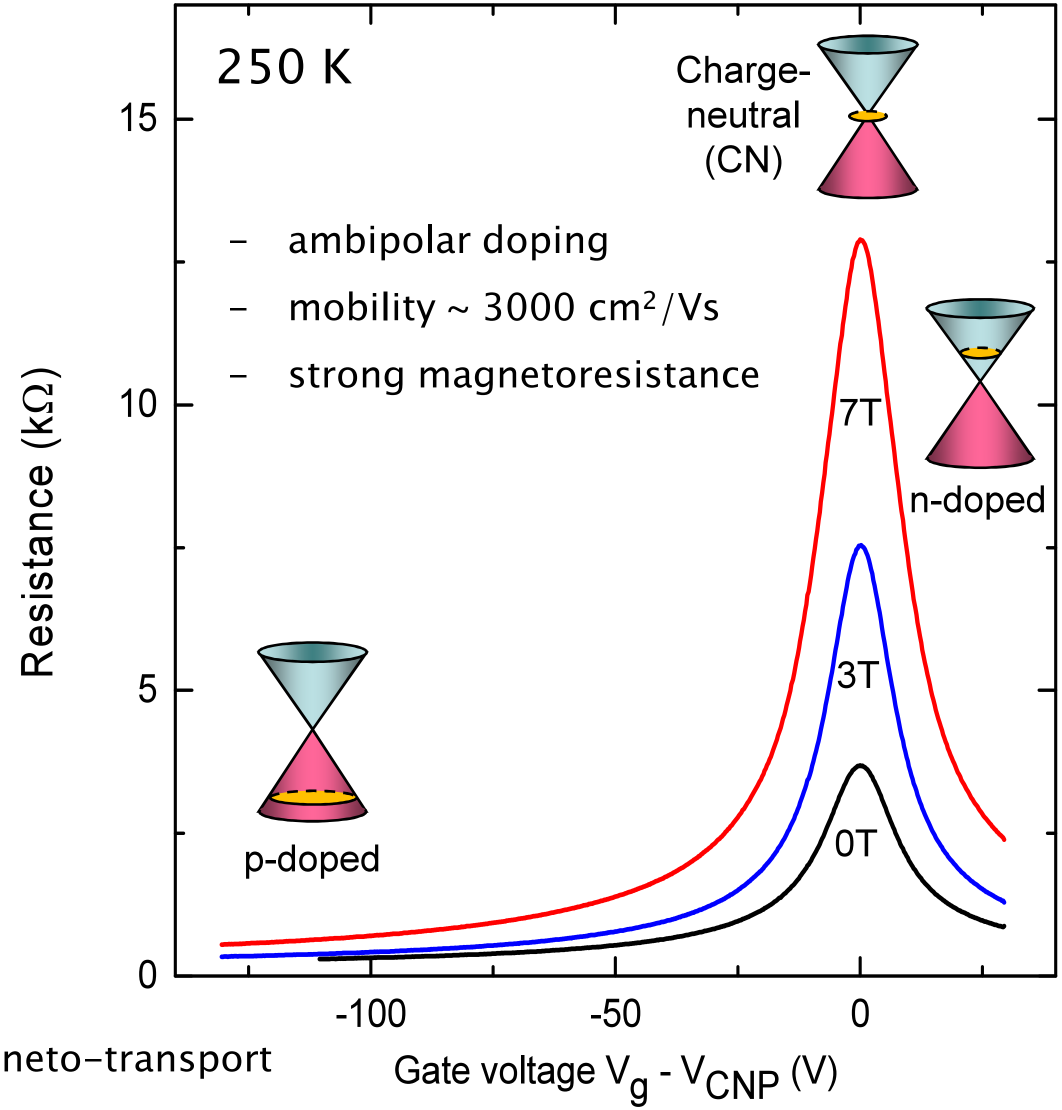

P. Q. Liu et al., Optica 2, 135 (2015)

Optical absorption in graphene

Graphite (HOPG)

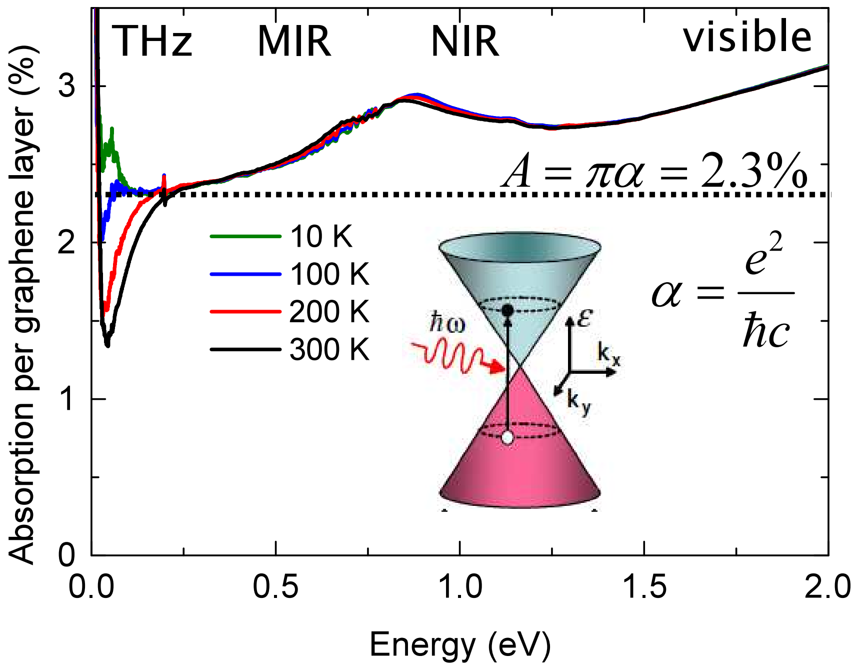

A. B. Kuzmenko et al., Phys. Rev. Lett. (2008)

Graphene membrane (visible)

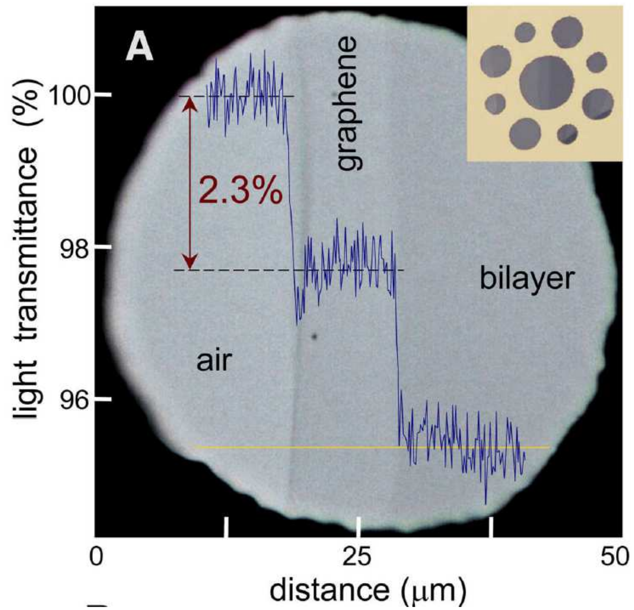

A.A. Nair et al., Science (2008)

Absorption in graphene is ‘universal’: 2.3%
but in the THz range it is much higher!!!
(thanks to Drude carriers)

Magneto-optical absorption of graphene: theory

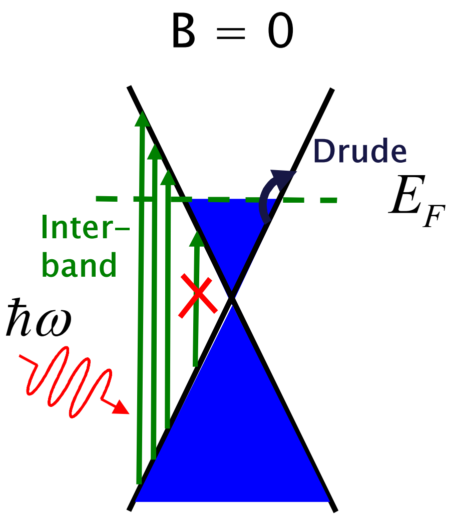

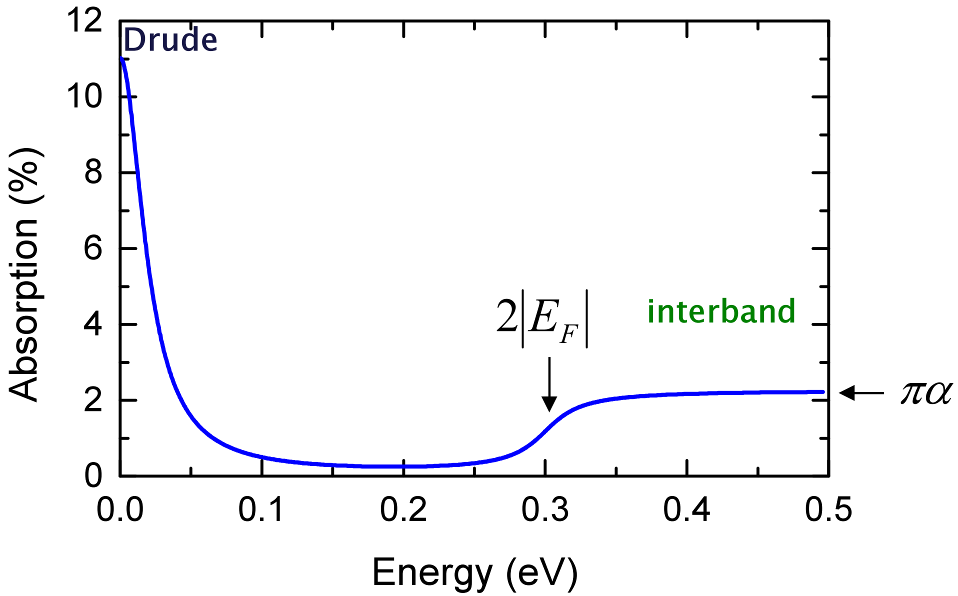

Magneto-optical absorption of graphene: theory

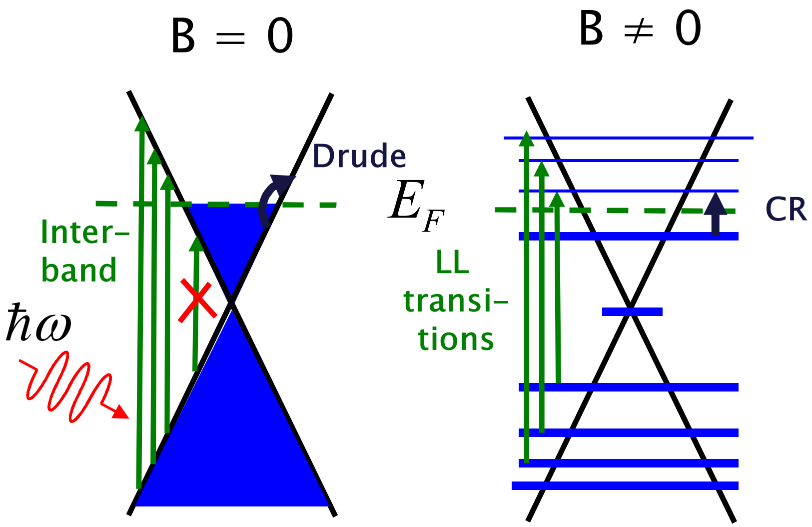

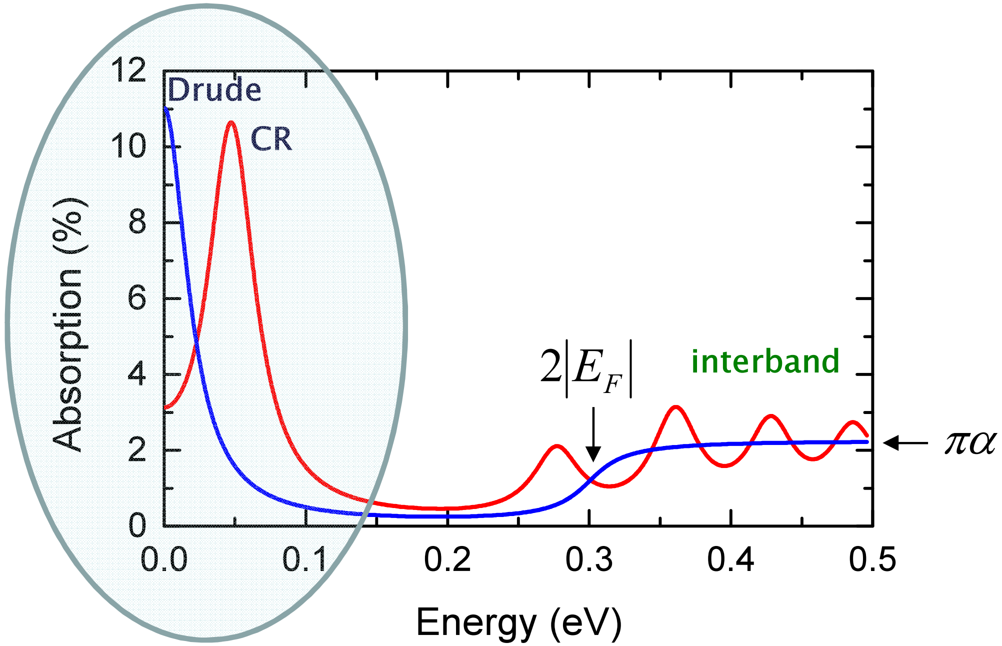

At high doping:'classical' cyclotron resonance (CR)

$$\sigma_{\pm}(\omega, B) = \frac{D}{\pi} \cdot \frac{i}{\omega \mp \omega_c(B) + i/\tau}$$

$$D = \frac{\pi n e^2}{m^*}$$ – Drude weight

τ – scattering time

$$\omega_c = \frac{eB}{m^*}$$ – cyclotron frequency

Dirac fermions*: $m^* = \frac{\hbar}{v_F}\sqrt{\pi n}$

$$D = \frac{e^2}{\hbar} v_F \sqrt{\pi n} \qquad \omega_c = \frac{eB}{\hbar} \frac{v_F}{\sqrt{\pi n}} sign(n)$$

Different from 2DEGs !

Ando (2002), Peres et al (2006)
Abergel & Falko (2007), Gusynin et al (2007)
Witowski (2010), Crassee (2011)

*interactions not included

Doping-dependent THz absorption in zero field

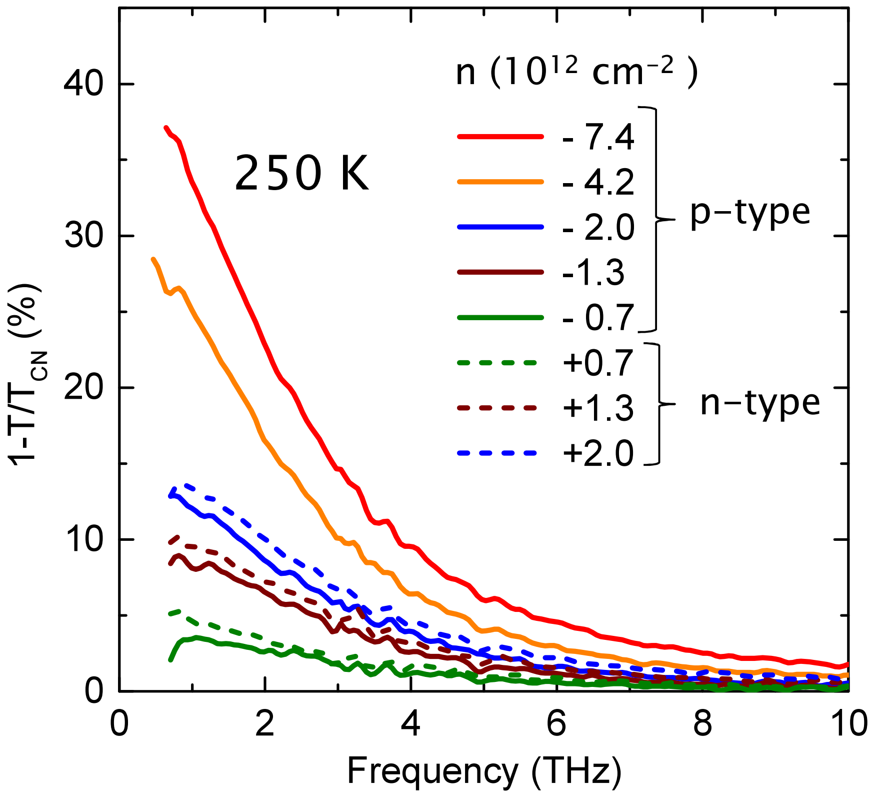

- ~40% absorption (<1THz)
- electron-hole symmetry

J.-M.Poumirol et al., Nature Communications, in press

Doping-dependent THz absorption in zero field

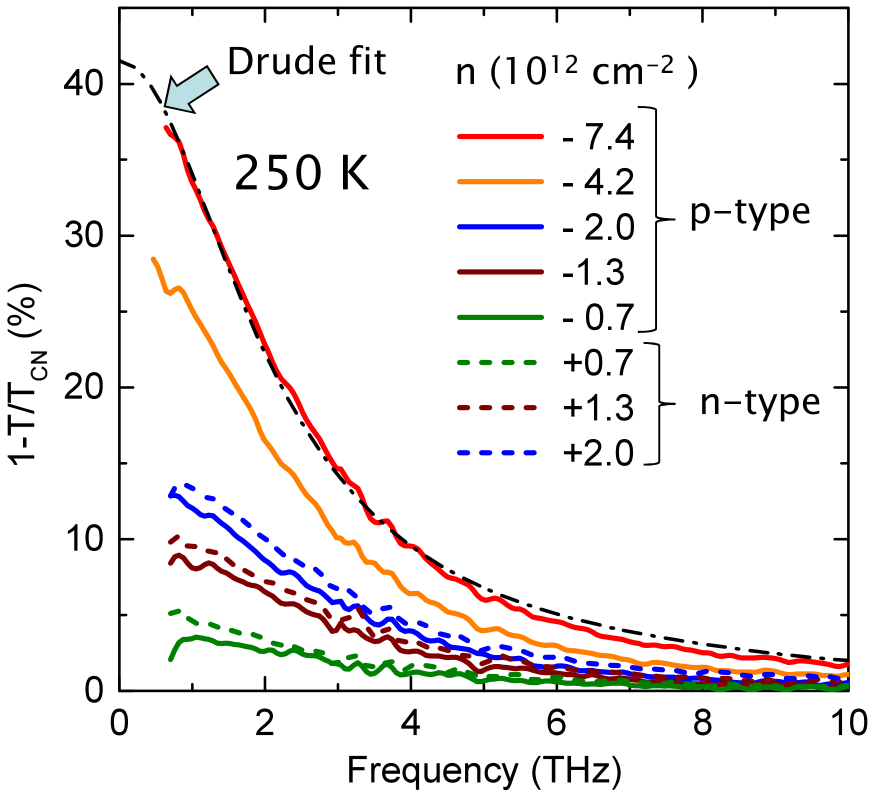

- ~40% absorption (<1THz)
- electron-hole symmetry
- Drude model works well

$$\sigma(\omega) = \frac{D}{\pi} \cdot \frac{i}{\omega + i/\tau}$$

J.-M.Poumirol et al., Nature Comm. (2017) DOI: 10.1038/ncomms14626

Doping-dependent THz absorption in zero field

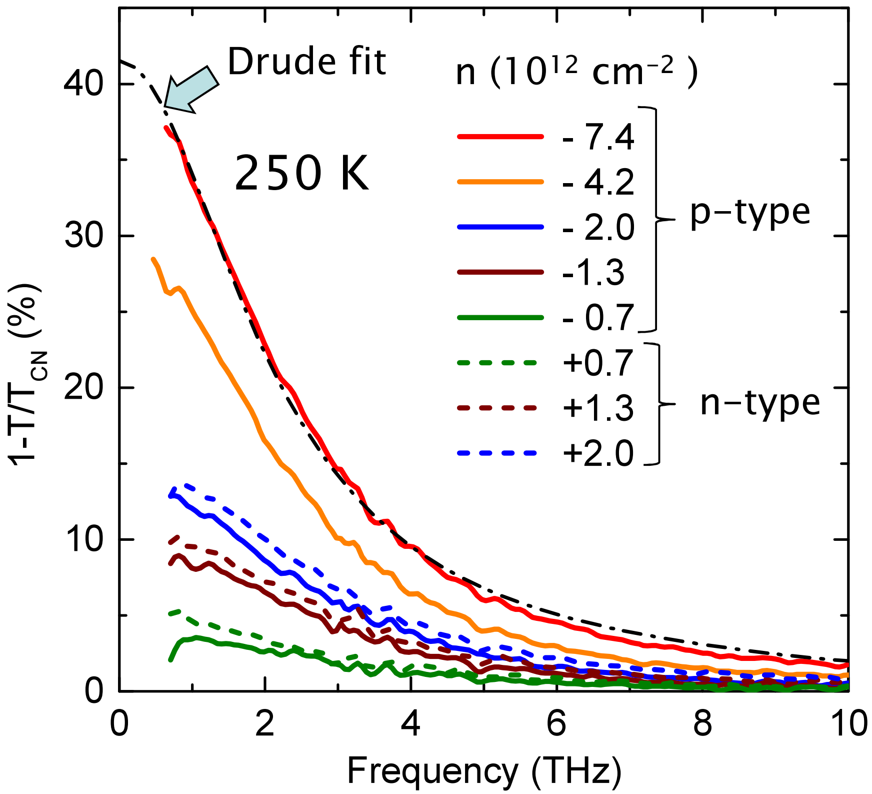

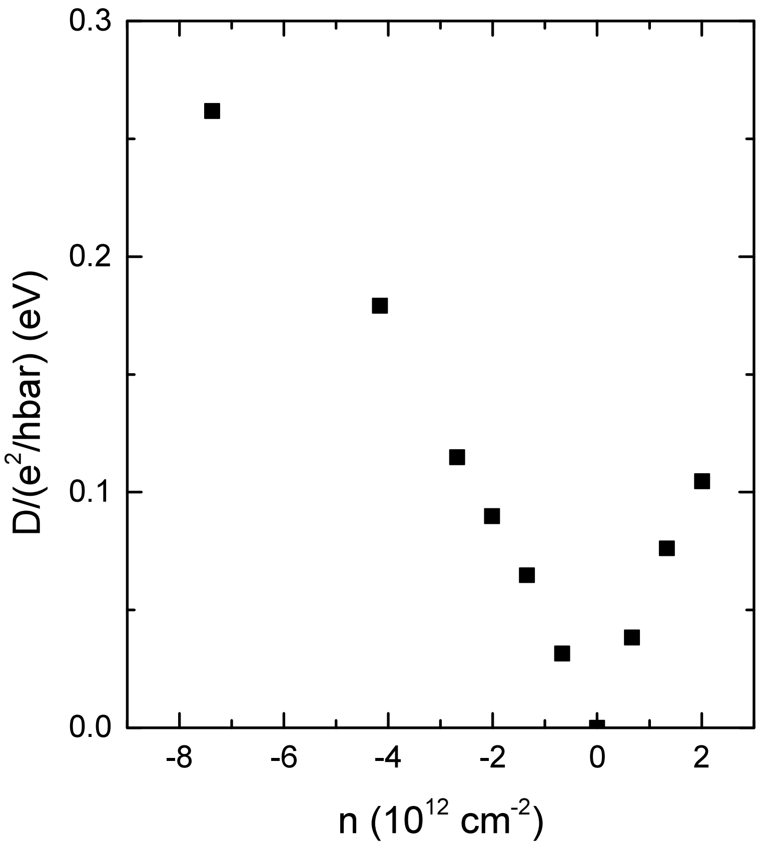

- ~40% absorption (<1THz)
- electron-hole symmetry
- Drude model works well

$$\sigma(\omega) = \frac{D}{\pi} \cdot \frac{i}{\omega + i/\tau}$$

J.-M.Poumirol et al., Nature Comm. (2017) DOI: 10.1038/ncomms14626

Doping-dependent THz absorption in zero field

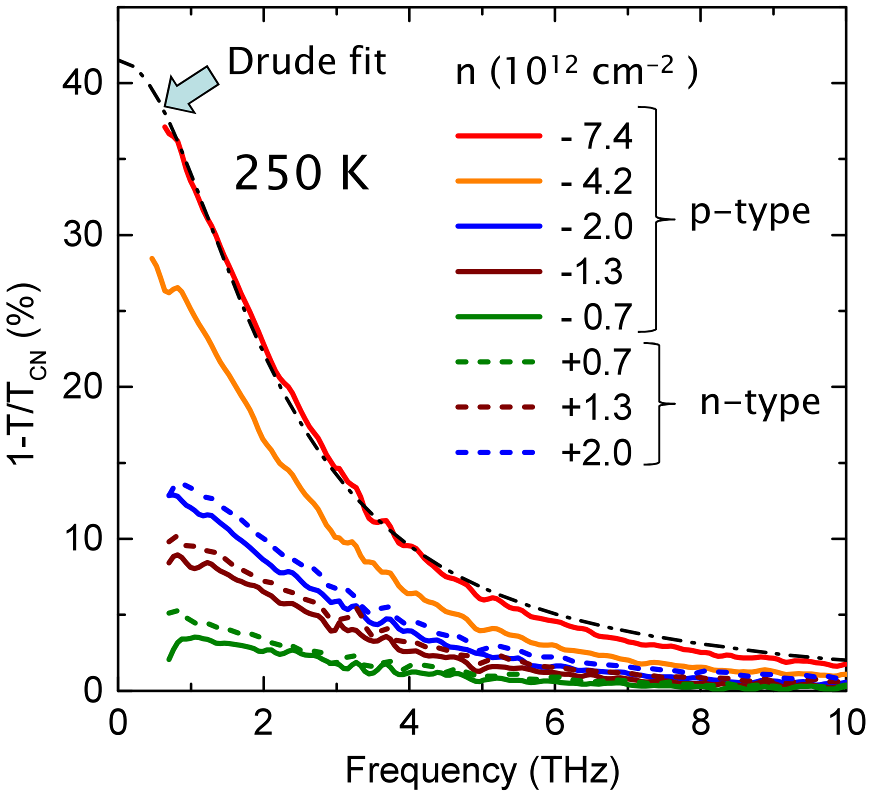

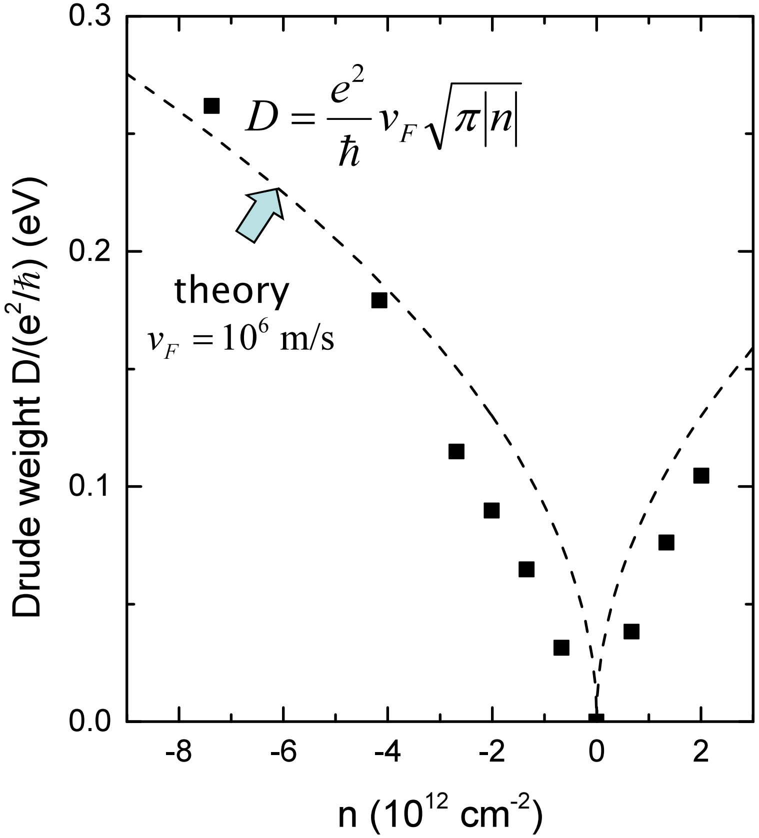

- ~40% absorption (<1THz)
- electron-hole symmetry
- Drude model works well

$$\sigma(\omega) = \frac{D}{\pi} \cdot \frac{i}{\omega + i/\tau}$$

J.-M.Poumirol et al., Nature Comm. (2017) DOI: 10.1038/ncomms14626

Doping-dependent THz absorption in zero field

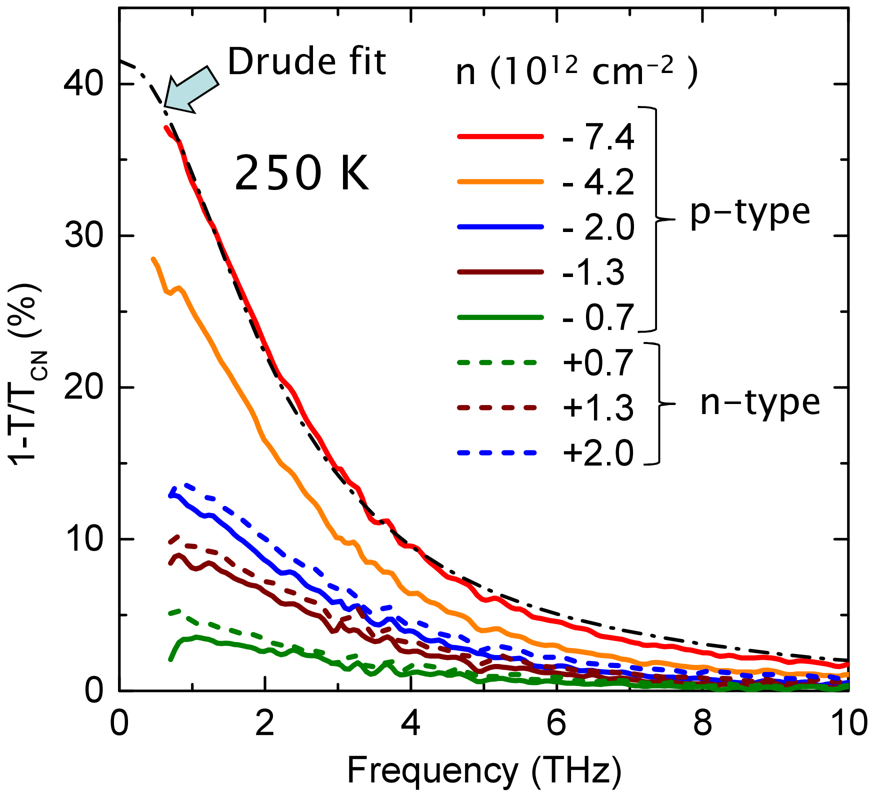

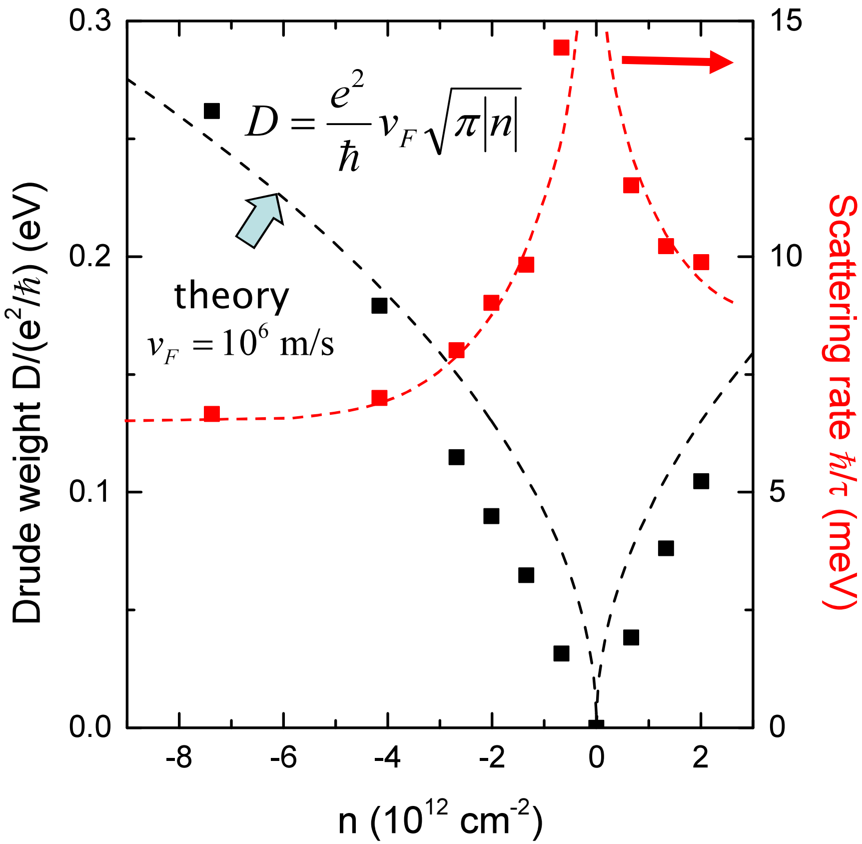

- ~40% absorption (<1THz)
- electron-hole symmetry
- Drude model works well
- Scattering by charged impurities (decreases with n)

$$\sigma(\omega) = \frac{D}{\pi} \cdot \frac{i}{\omega + i/\tau}$$

J.-M.Poumirol et al., Nature Comm. (2017) DOI: 10.1038/ncomms14626

B-field dependence of THz effects (high doping)

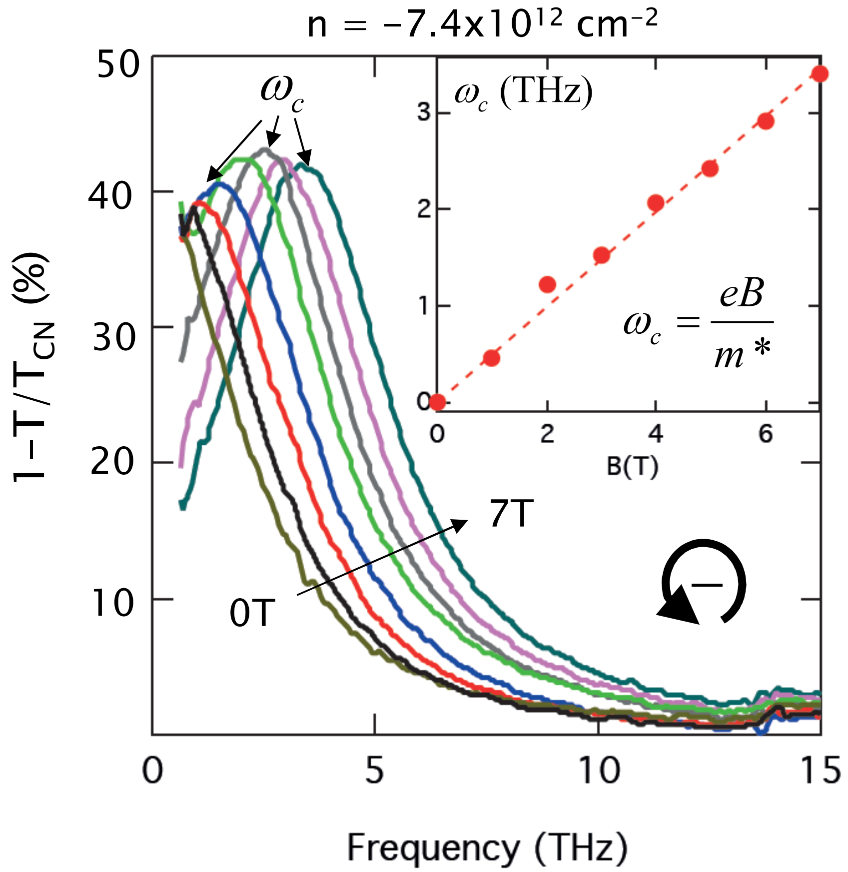

- Absorption >40% at 3 THz
- Cyclotron frequency is B-linear

J.-M.Poumirol et al., Nature Comm. (2017) DOI: 10.1038/ncomms14626

B-field dependence of THz effects (high doping)

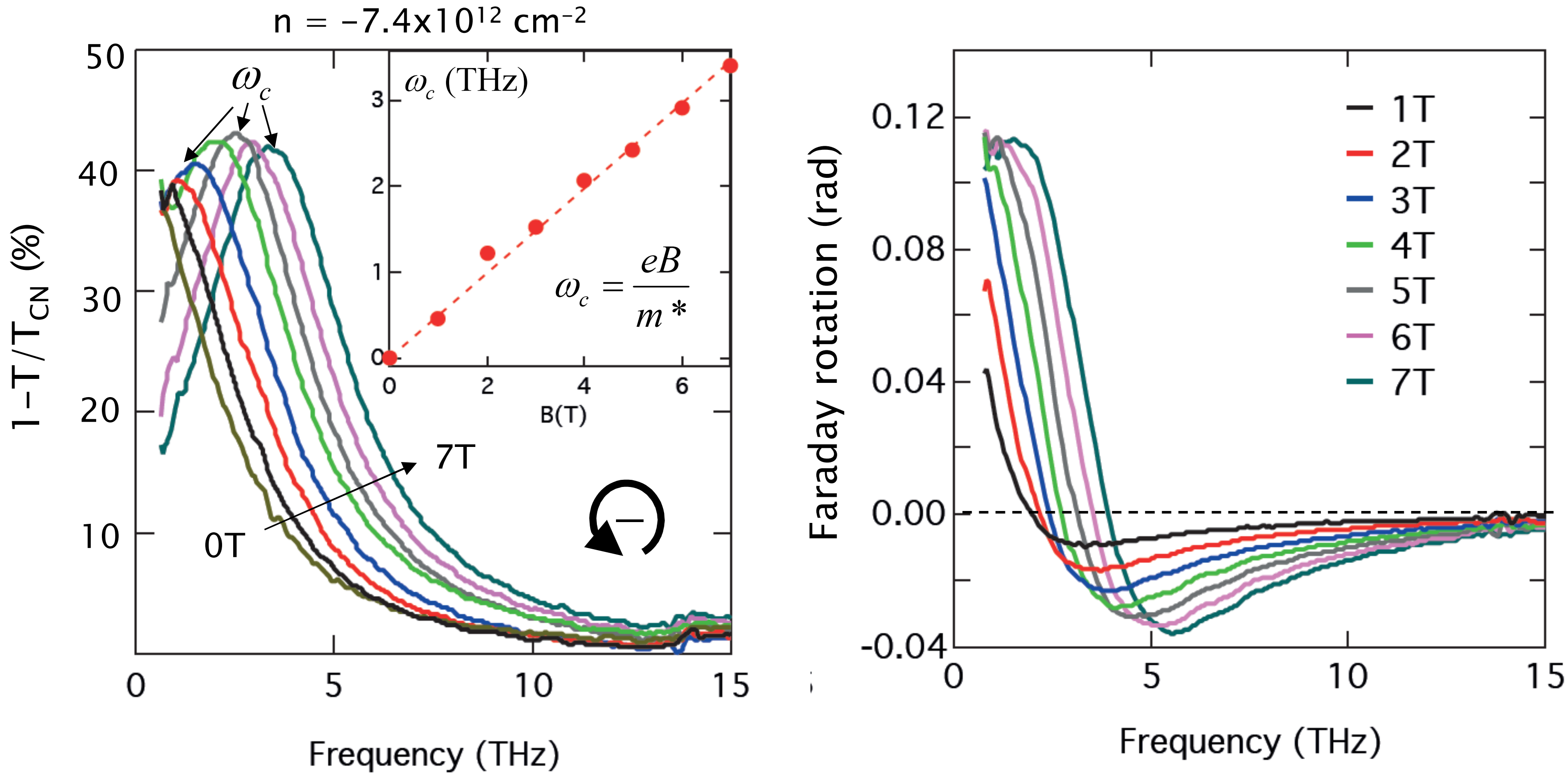

- Absorption >40% at 3 THz
- Cyclotron frequency is B-linear

- Faraday rotation θ_F >0.1 rad (6 deg)

Similar to epitaxial graphene on SiC:
I. Crassee *et al.* Nature Phys.**7**, 48 (2011)

J.-M.Poumirol et al., Nature Communications, in press

Doping dependence of MO THz effects

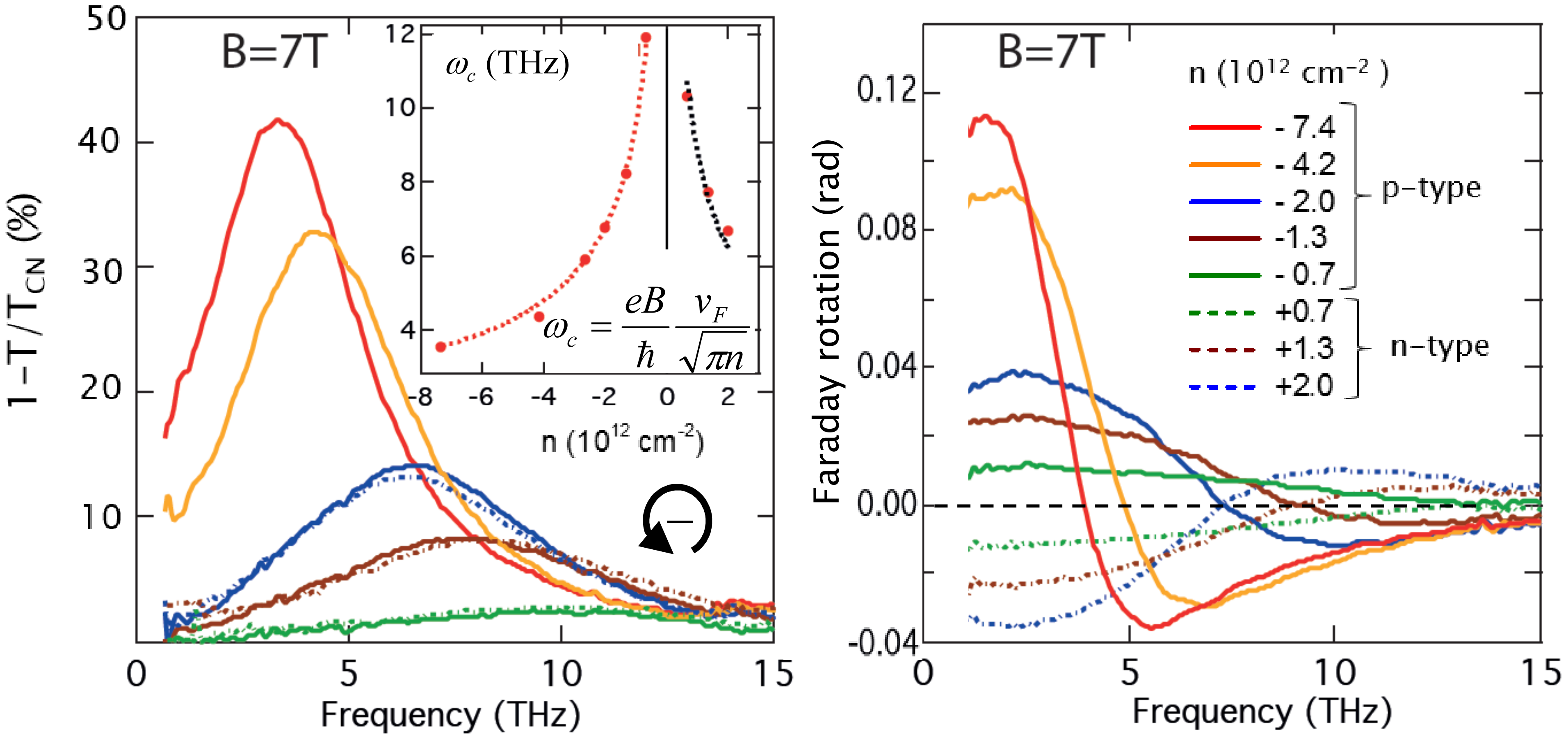

- Cyclotron frequency $\omega_c \sim n^{-1/2}$
- ω_c >10 THz can be reached !

Drastically different from 2DEGs!

J.-M.Poumirol et al., Nature Comm. (2017) DOI: 10.1038/ncomms14626

Electric control of MCD and Faraday rotation

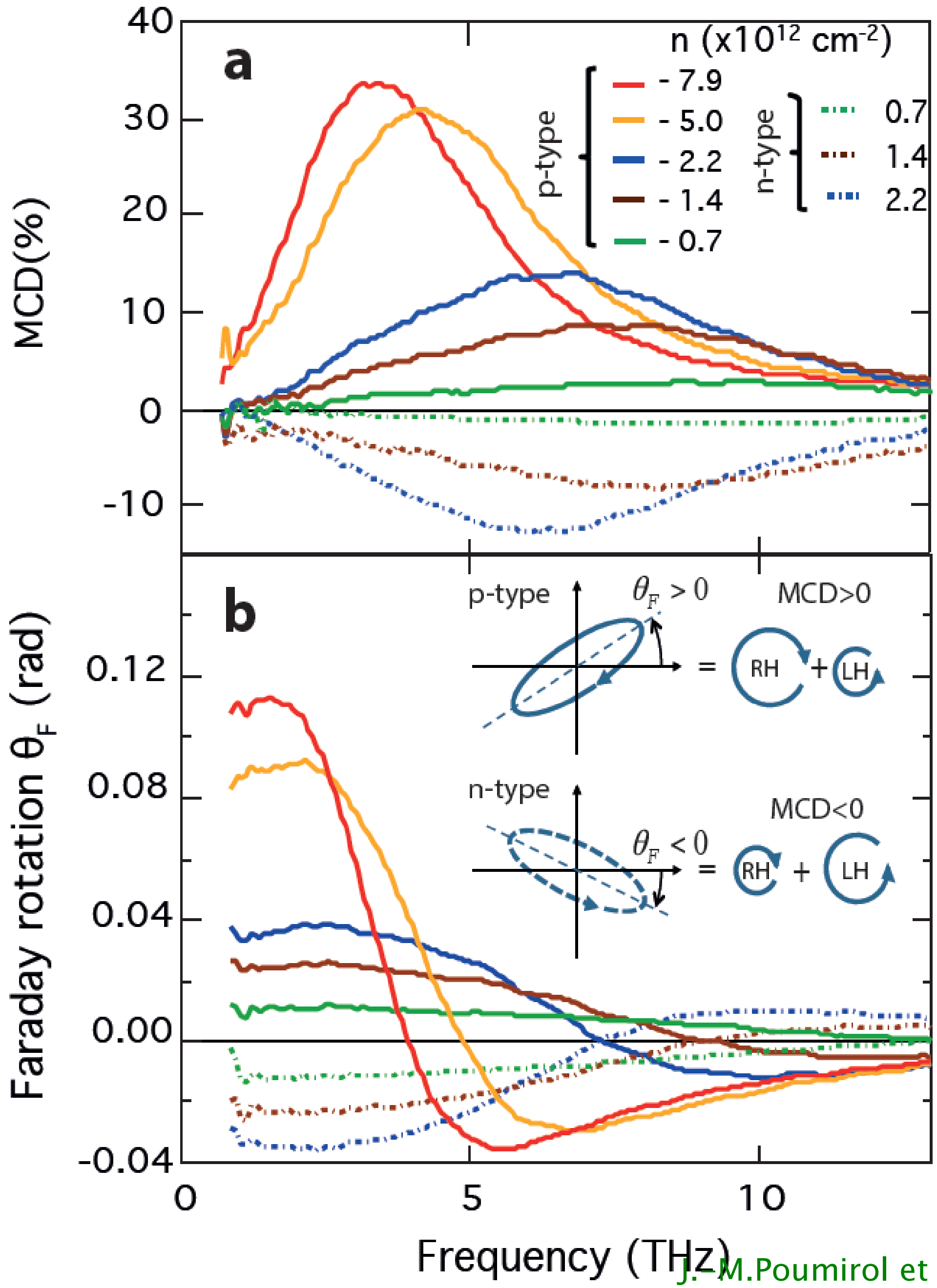

– Magnetic circular dichroism and Faraday rotation can be inverted <u>electrostatically</u> !

– Electric control of a magnetic effect !

– Potentially new MO device functionalities !

J.-M.Poumirol et al., Nature Comm. (2017) DOI: 10.1038/ncomms14626

Graphene antidots: fabrication and transport

Square array of
micron-size holes (antidots)

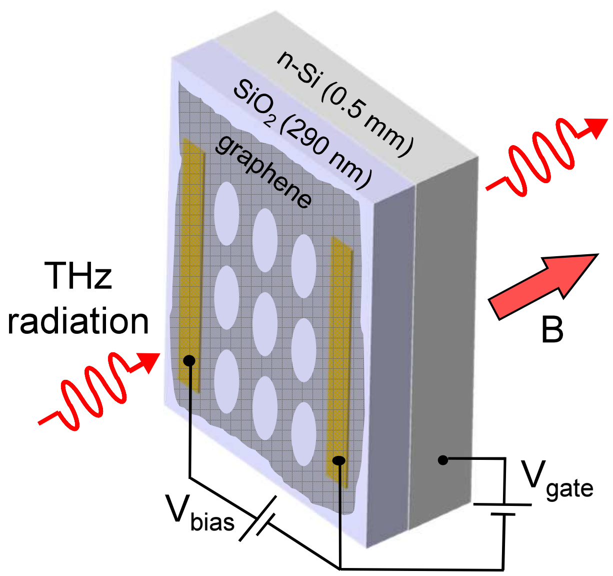

patterned by deep-UV
photolithography
and O_2-plasma etching

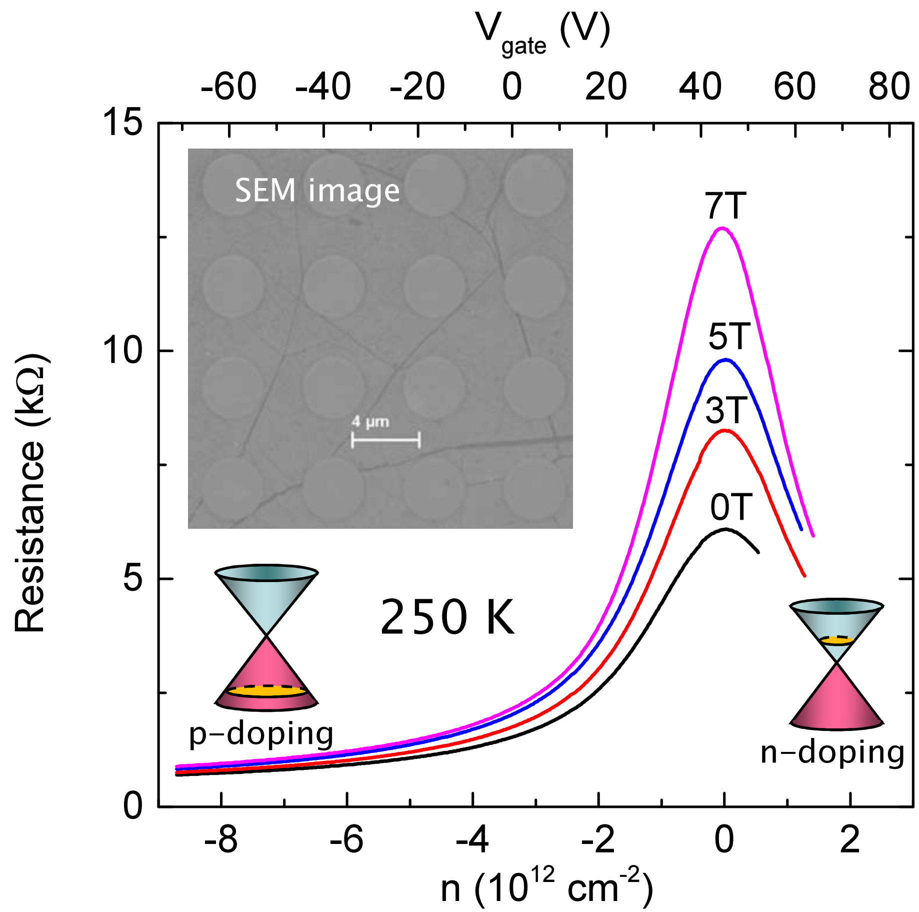

P. Q. Liu et al., Optica 2, 135 (2015)

Graphene antidots: zero-field THz absorption

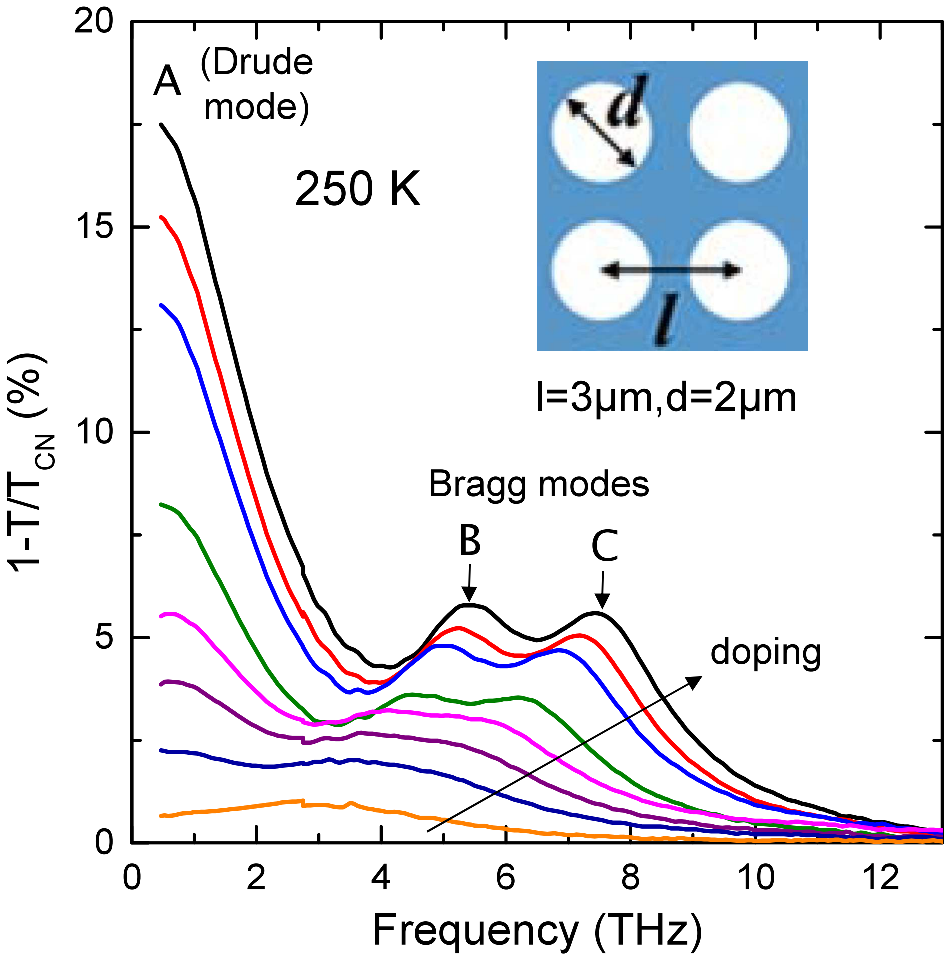

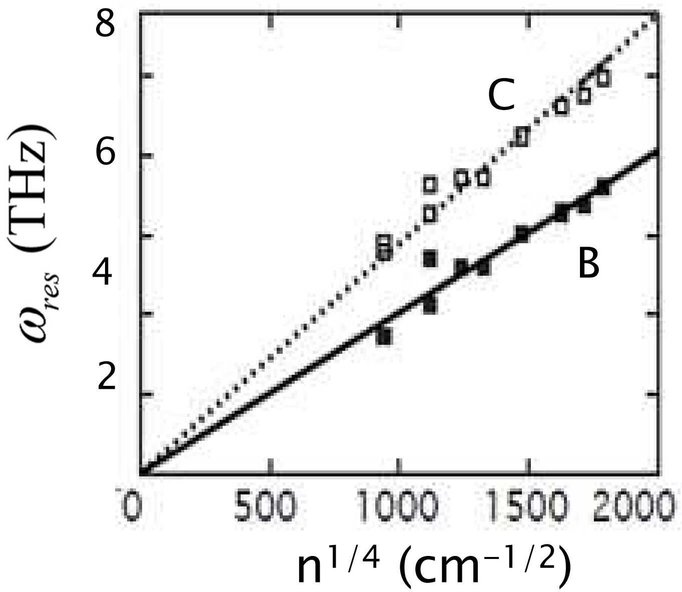

2D plasmon dispersion: $\omega_{\rm pl}(n,q) = \left(\dfrac{4\pi n e^2 q}{m(\varepsilon_{sub}+1)} \right)^{1/2}$

In graphene $m \propto n^{1/2}$ $\Rightarrow$ $\omega_{\rm pl}(n,q) \propto n^{1/4} q^{1/2}$

P. Q. Liu et al., Optica 2, 135 (2015)

J.-M.Poumirol et al., Nature Comm. (2017) DOI: 10.1038/ncomms14626

Graphene antidots: THz magneto-absorption

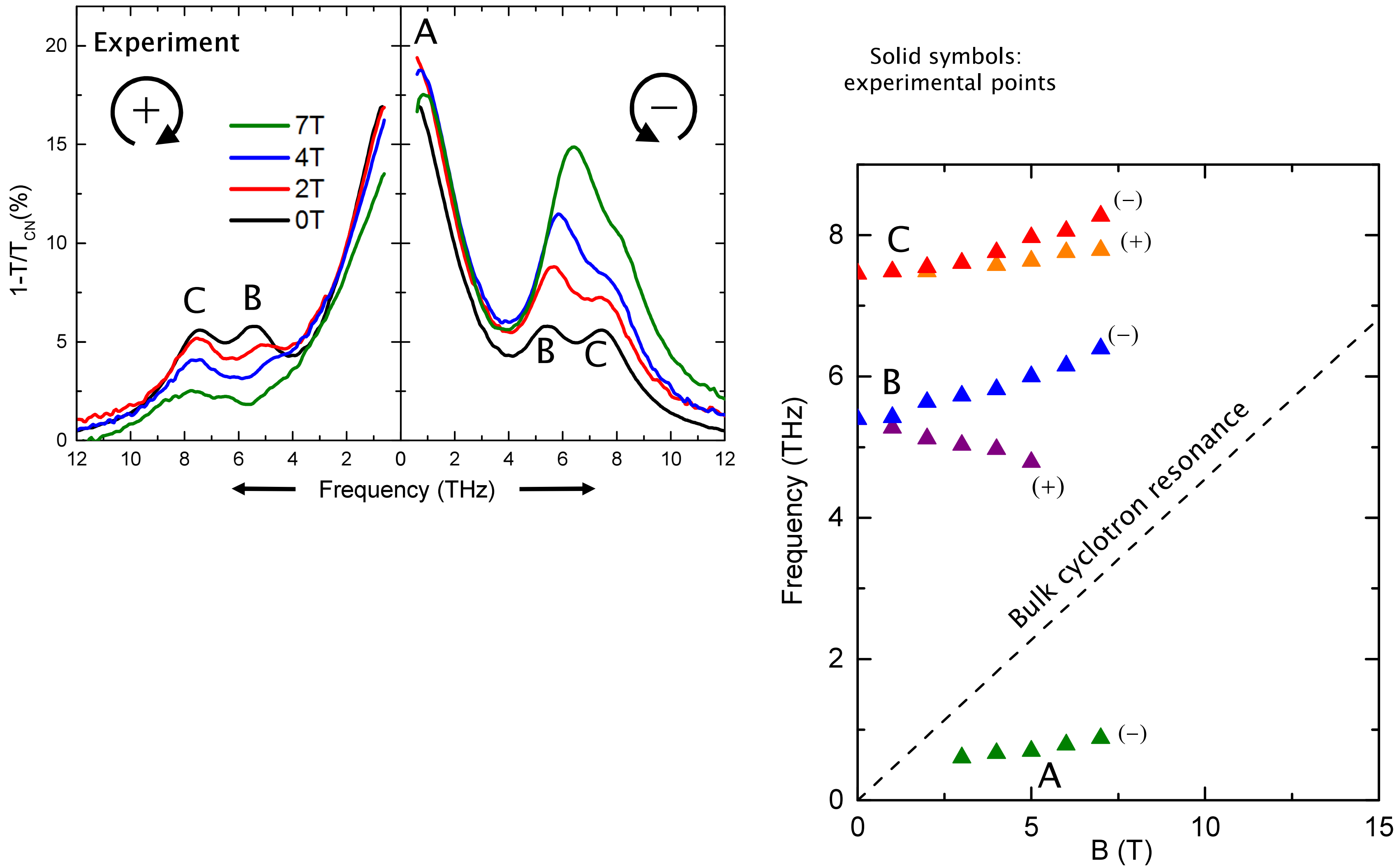

J.-M.Poumirol et al., Nature Communications, in press

Graphene antidots: THz magneto-absorption

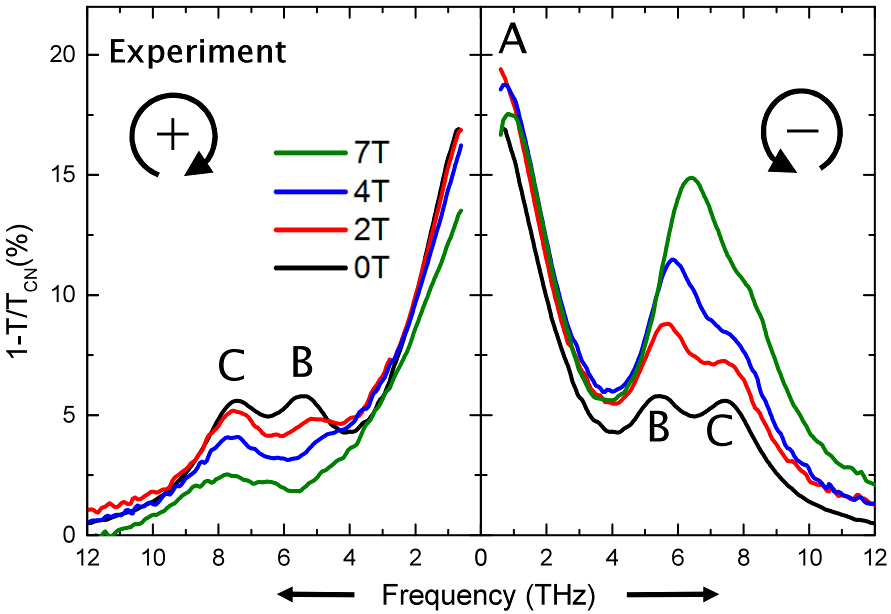

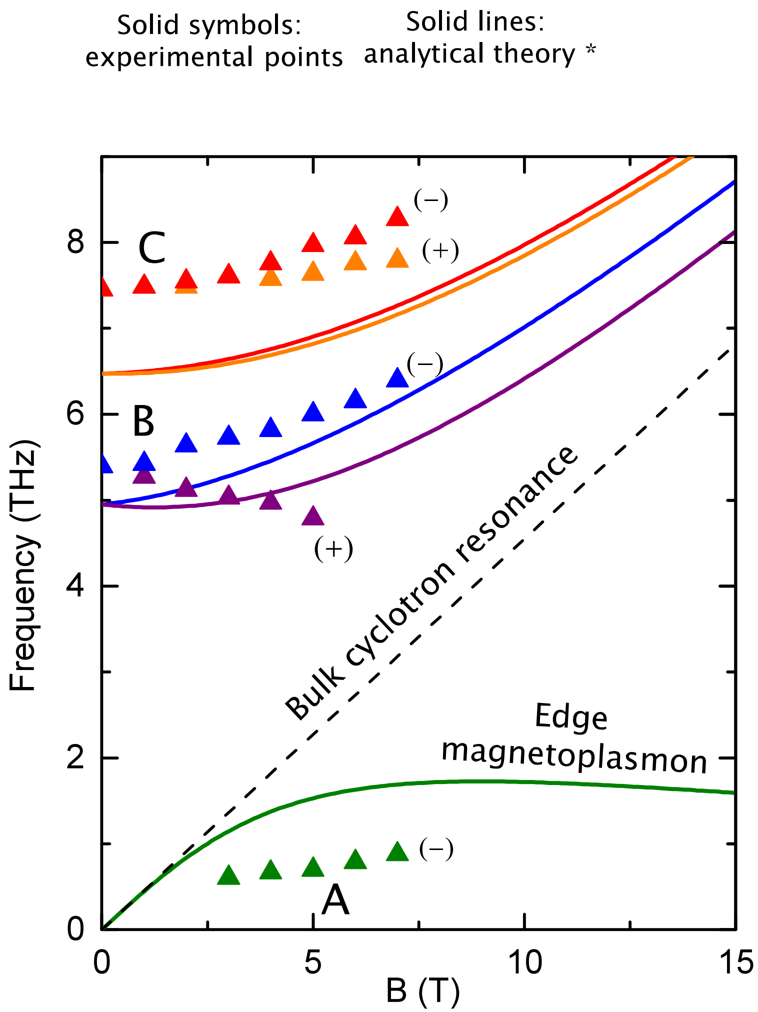

*S.A.Mikhailov and V.A. Volkov, Phys. Rev. B 52, 17260 (1995)
*S.A.Mikhailov, Phys. Rev. B 54, 14293 (1996)

J.-M.Poumirol et al., Nature Communications, in press

Graphene antidots: THz magneto-absorption

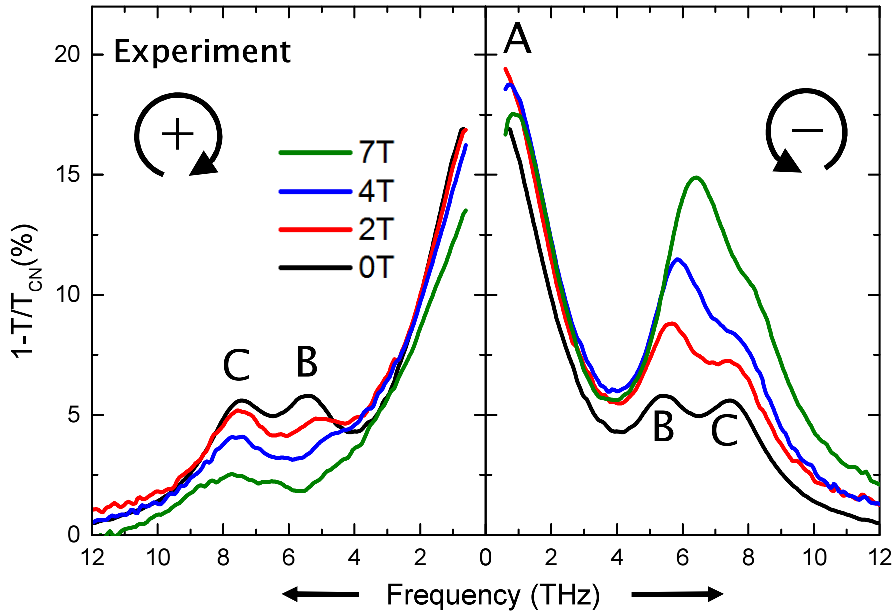

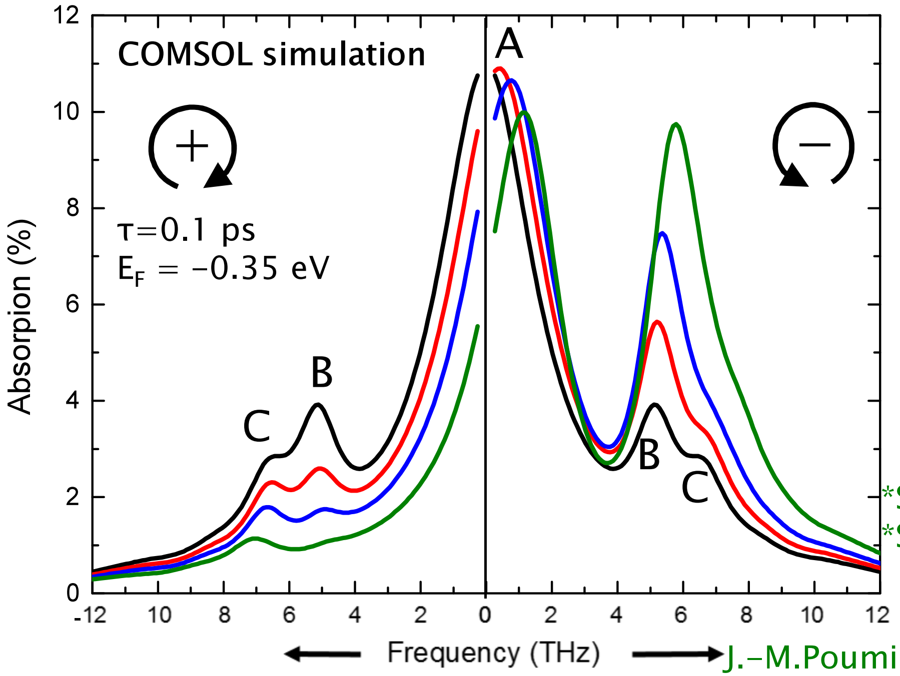

Solid symbols: experimental points

Solid lines: analytical theory *

Open circles: COMSOL simulation

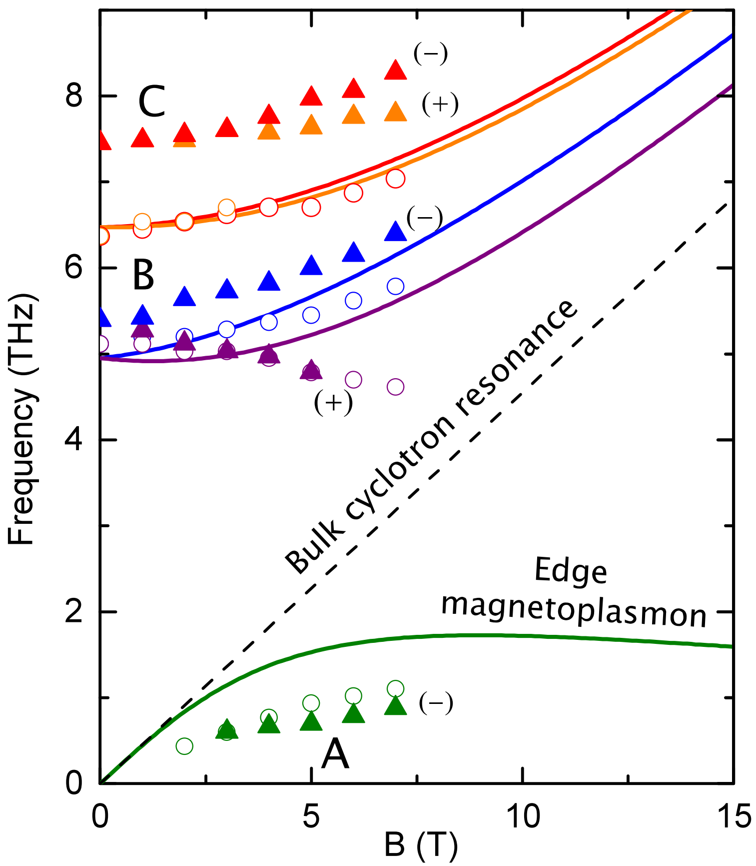

*S.A.Mikhailov and V.A. Volkov, Phys. Rev. B 52, 17260 (1995)

*S.A.Mikhailov, Phys. Rev. B 54, 14293 (1996)

J.-M.Poumirol et al., Nature Comm. (2017) DOI: 10.1038/ncomms14626

Graphene antidots: THz magneto-absorption

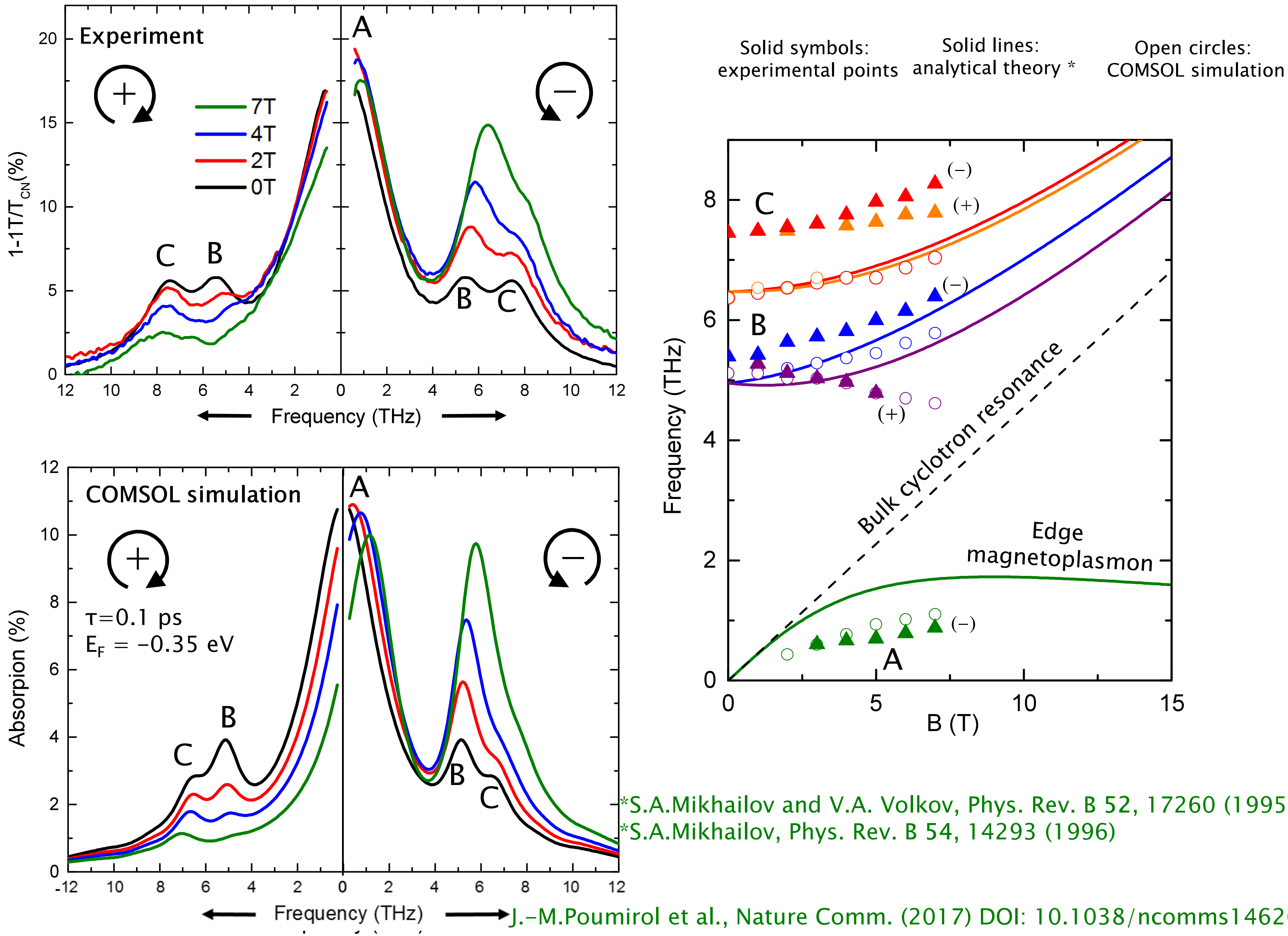

*S.A.Mikhailov and V.A. Volkov, Phys. Rev. B 52, 17260 (1995)
*S.A.Mikhailov, Phys. Rev. B 54, 14293 (1996)

J.-M.Poumirol et al., Nature Comm. (2017) DOI: 10.1038/ncomms14626

Simulated field profiles in graphene antidots

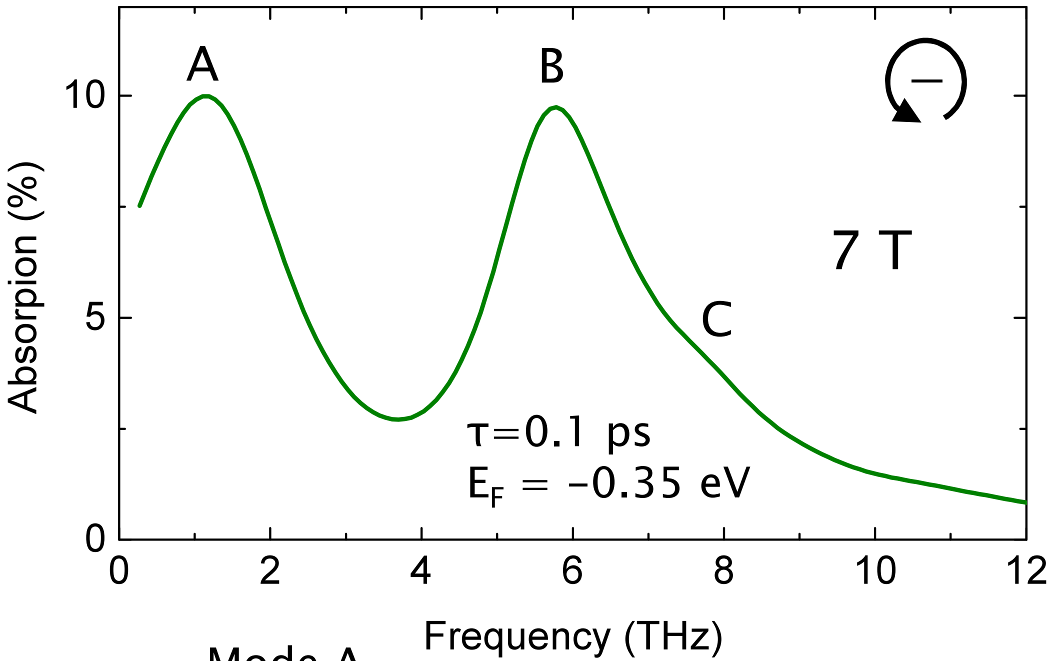

Rich graphene magneto-plasmon physics !

Mode A (edge magneto-plasmon)

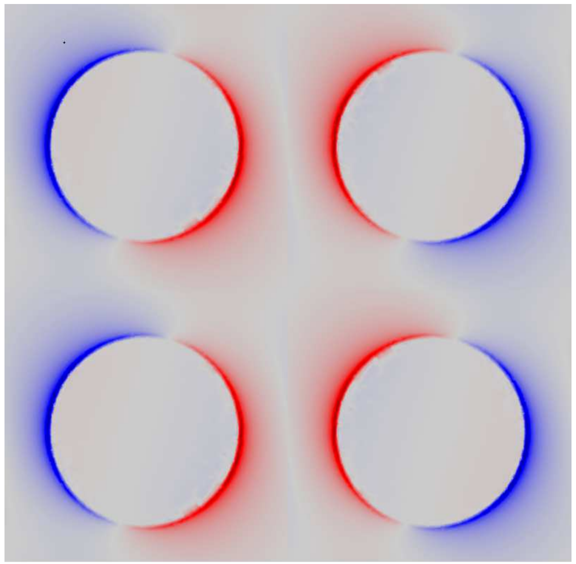

Mode B

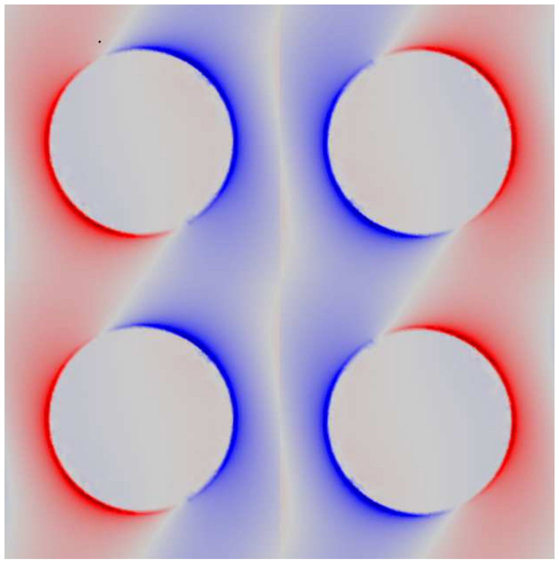

Mode C

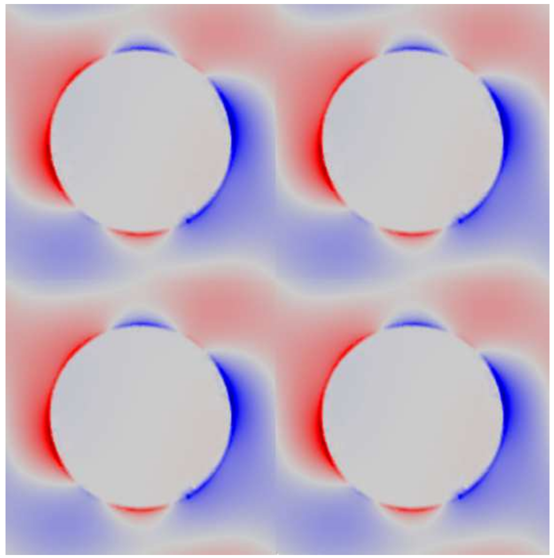

Faraday rotation in continuous and patterned graphene

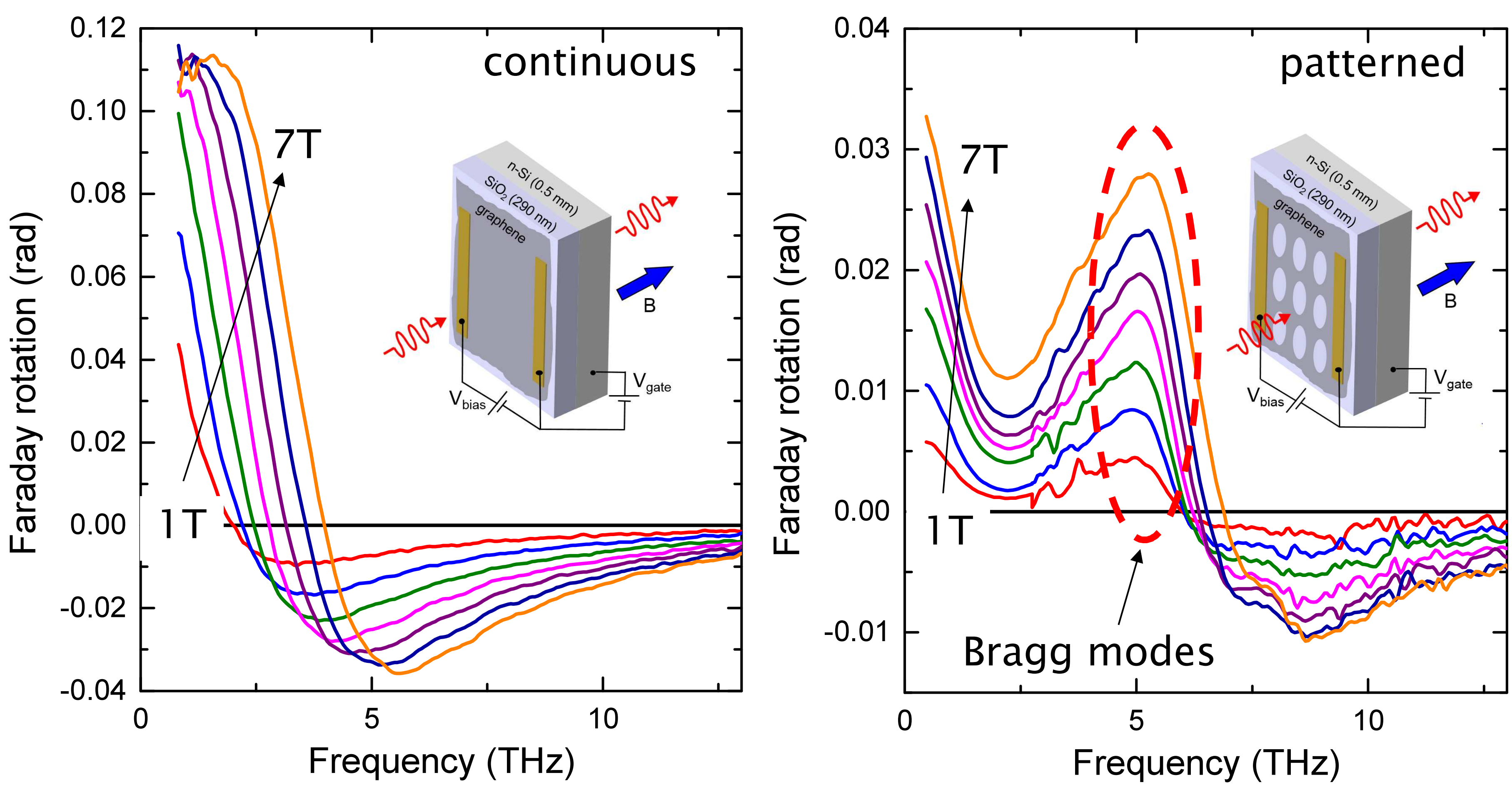

Patterning blue-shifts frequency of maximum Faraday rotation

J.-M.Poumirol et al., Nature Comm. (2017) DOI: 10.1038/ncomms14626

Passive graphene-based THz elements

THz technology is lacking efficient passive devices:

- Reciprocal: modulators, polarization converters etc.
- Non-reciprocal: isolators, circulators etc.

Graphene:

- Very efficient for manipulating THz waves
- Ultrathin (magneto-THz effects occurs in an atomically thin layer)
- Electrostatically switchable -> new functionalities

Optical isolator (diode, valve etc.)

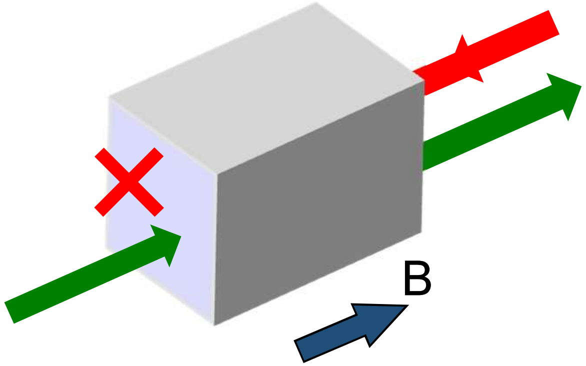

- Critical element in many applications (communications, lasers, optical computing etc.)
- Uses non-reciprocal magneto-optical effects (Faraday rotation or magnetic circular dichroism)
- Often very bulk (a few cm thick)
- Difficult to invert

Microwave (< 150 GHz)
(based on ferrites)

THz
(1–10 THz)

Nothing !!!

MIR-visible (> 15 THz)
(based on magnetic glasses)

First prototype THz graphene-based isolator

3 graphene layers
by PMMA

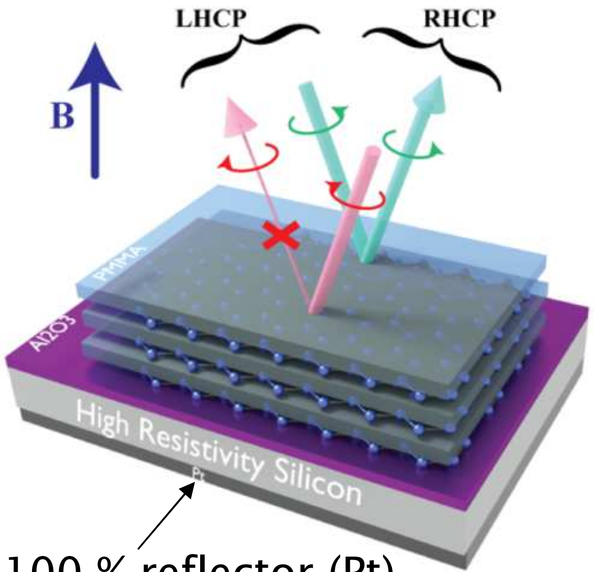

100 % reflector (Pt)

Fabry-Perot in Si layer (10 μm)

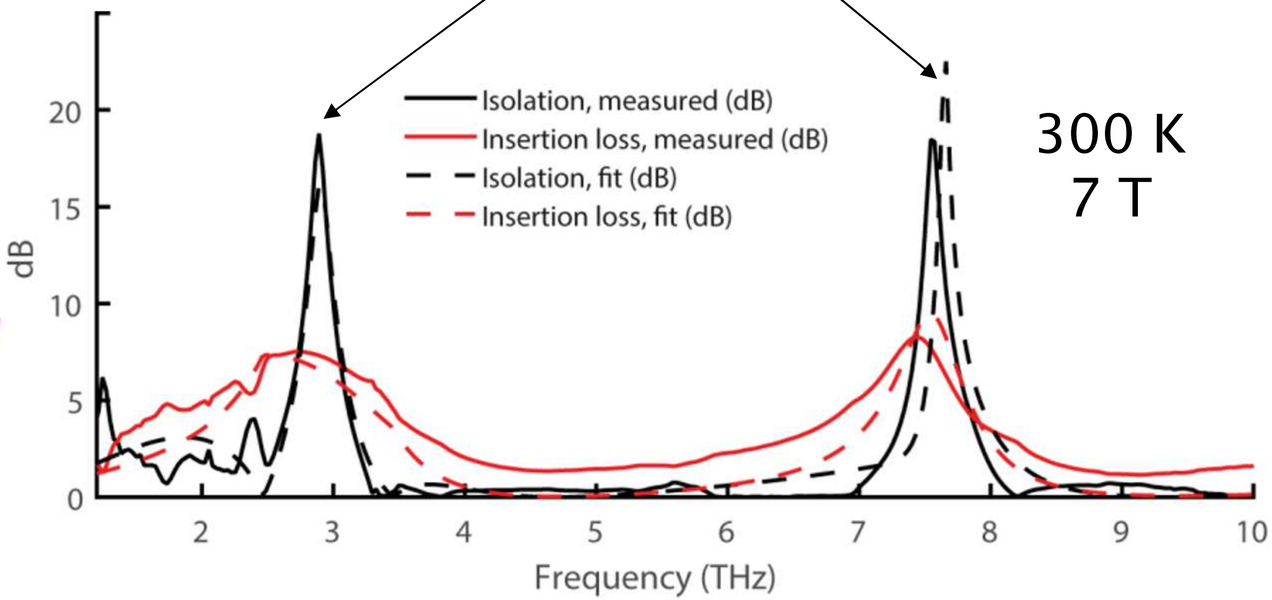

300 K
7 T

- isolation >18 dB
- insertion loss <7 dB
- operates in reflection

M. Tamagnone et al., Nature Commun. **7**, 11216 (2016)

Reducing the B-field is imperative for applications

7 T

<1.5 T

Summary

- Handedness resolved magneto-infrared spectroscopy

  J. Levallois et al., Rev. Sci. Instrum. **86**, 033906 (2015)

- Suppressed MCD and valley-polarized absorption in Bi

  P.J. de Visser, J. Levallois *et al.* Phys. Rev. Lett. 117, 017402 (2016)

- Electrically controlled terahertz MCD and FR in graphene

  J.-M.Poumirol et al., Nature Communications, in press

- Towards graphene-based magneto-optical THz devices

  M. Tamagnone et al., Nature Commun. **7**, 11216 (2016)

PhD and Postdoc positions available !!!

www.graphene-flagship.eu

GRAPHENE FLAGSHIP

UNIVERSITÉ DE GENÈVE

FNSNF

FONDS NATIONAL SUISSE DE LA RECHERCHE SCIENTIFIQUE